Trebuchet versus Flinger:
Millennial mechanics and bio-mechanics problems

William G. Harter
Department of Physics
University of Arkansas
Fayetteville, AR 72701

The *trebuchet* or *ingenium* was introduced to Western Civilization before the tenth century. It was used as a devastating weapon until just before the time of Galileo. After this it seems to be all but forgotten until its recent recreation by a few engineers and medievalists. We show here that the trebuchet also deserves the attention of physicists and others who study mechanics. The study of the trebuchet is a rich source of analogies between topics ranging from parametric resonance and quantum band theory to the bio-mechanics of a tennis or golf stroke. With modern technology, the possibility of a supersonic trebuchet arises.

1. Introduction

The *trebuchet* or *ingenium* [1,2] was a super-catapult invented in China about 400BC and improved during the Mongol empires. Between the time of the Crusades and the fifteenth century this device became a large and fearsome weapon with some ingenia able to throw several-ton projectiles hundreds of feet. (The title *engineer* and term *engine* seem to have originated with the *ingeniators* [3] and their ingenia.)

A trebuchet has a heavy weight fixed at one end of a large lever or beam on a strong fulcrum with a second smaller lever or rope swinging like a pendulum from the opposite end of the big beam. A sketch in Fig. 1 shows a simplified trebuchet to be little more than a student's swiveling desk lamp with springs removed so, if the big counterweight *M* were to fall, it might launch the lamp's light bulb *m* through a window. (Don't try this at home!)

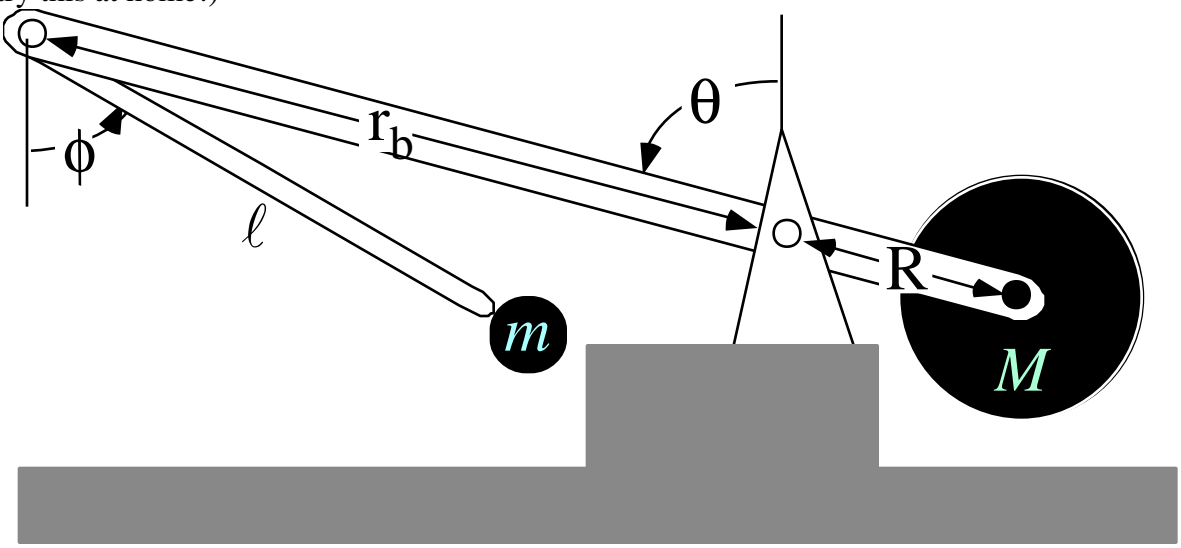

Fig. 1 The elementary ground-fixed Trebuchet

Obviously, this device is dangerous and therein lies its initial appeal to modern physics students! Some engineers and medievalists [1,2] have received worldwide attention by building trebuchets that heave pianos, cars, rocks (as well as some thrill-crazed people!) hundreds of feet. In addition, as will be shown below, this ancient weapon is incredibly relevant and helpful to the study of a number of areas of physics and mathematics not the least of which is elementary classical mechanics and sports bio-mechanics. In spite of this, there is little mention of this device in the physics literature and virtually no treatment of it in mechanics texts.[4]

Recently, to begin correcting this omission, we began our junior and graduate mechanics course [5] by imagining that Galileo is contracted by generals to apply his new *Scie'ncia Mecha'nica* to analyze and improve their five hundred-year-old trebuchet. (It is important to emphasize that there is no evidence that Galileo ever studied a trebuchet or was ever a consultant to the Vatican military industrial complex. Furthermore, by 1500, cannon metal had improved to the point that ordnance began, at last, to outperform trebuchets. The last recorded trebuchet attack was a disastrous fiasco (discussed below) in the siege of Montezuma by Cortez in 1521.)

We can ask, "What would Galileo have to do to improve on 500 years of trial-and-error engineering?" In other words, we imagine the generals asking, "What good is this new physics stuff?" The answer, it appears at first cut, is, "Not much!" It seems that poor Galileo would have to invent the next 500 years of mechanics, that is, do the work of Newton, Lagrange, Hamilton, just to name a few, and then, on top of all that, invent and build a computer to solve some fairly dicey non-linear differential equations.

Galileo is famous for analyzing the small-amplitude pendulum, but that is just a tiny part of the trebuchet motion: the swinging of the spent rope after a launch as sketched in Fig. 2b. The actual launch sketched in Fig. 2a is a large-amplitude non-linear coupled motion with problems that challenge even modern mechanists. Our current mechanics texts mostly emphasize more easily solvable problems such as a small-amplitude (linear) coupled pendulums. (A trebuchet trembling around its up-and-down resting position in Fig. 2b might be so analyzed.) Therefore, perhaps, it is easy to rationalize trebuchet-avoidance in physics texts. A traditional physicist might dismiss the trebuchet problem with a huge puff of smelly pipe smoke and harumpf, "It's just engineering!". Or, a younger physicist, after a sip of Perrier, might sniff, "We don't do war machines here anymore!"

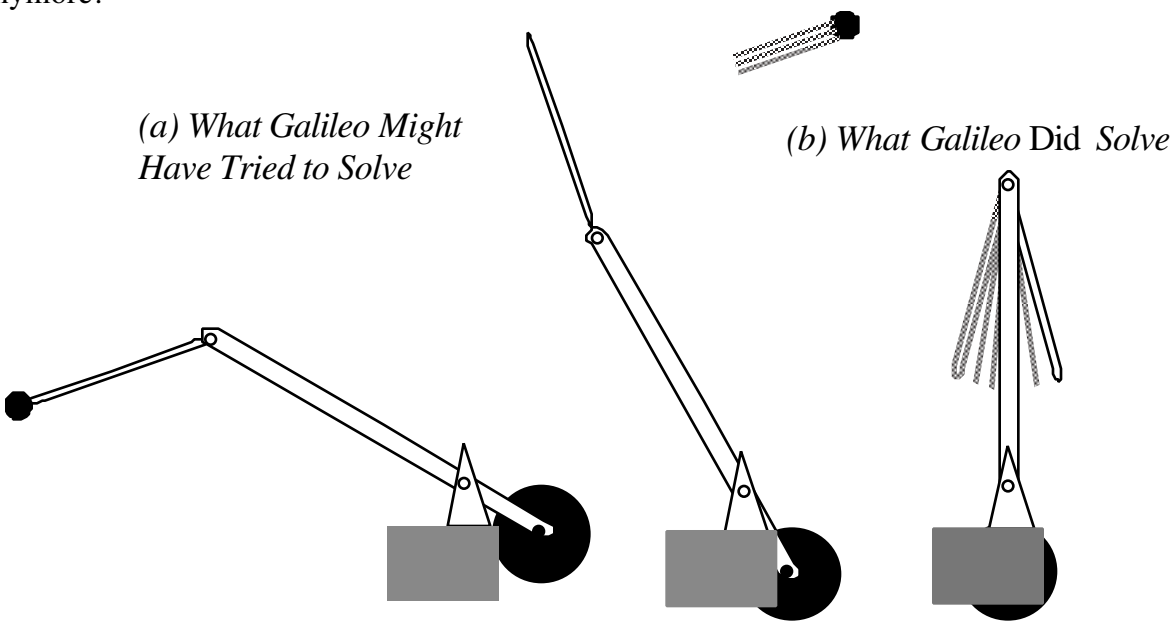

Fig. 2 Galileo's Supposed Problem: Solve the trebuchet

2. An old problem: Why is it still relevant physics?

The trebuchet represents an important problem that has affected human life day in and day out for thousands of years. It is not so much the war machines themselves, though they did have bad effects such as spreading black plague when they heaved victims' corpses into castles. Rather, it is the motion of the trebuchet that duplicates human throwing, chopping, digging, cultivating, and reaping motions in Fig. 2(c)

(a) Early Human Agriculture and Infrastructure Building Activity

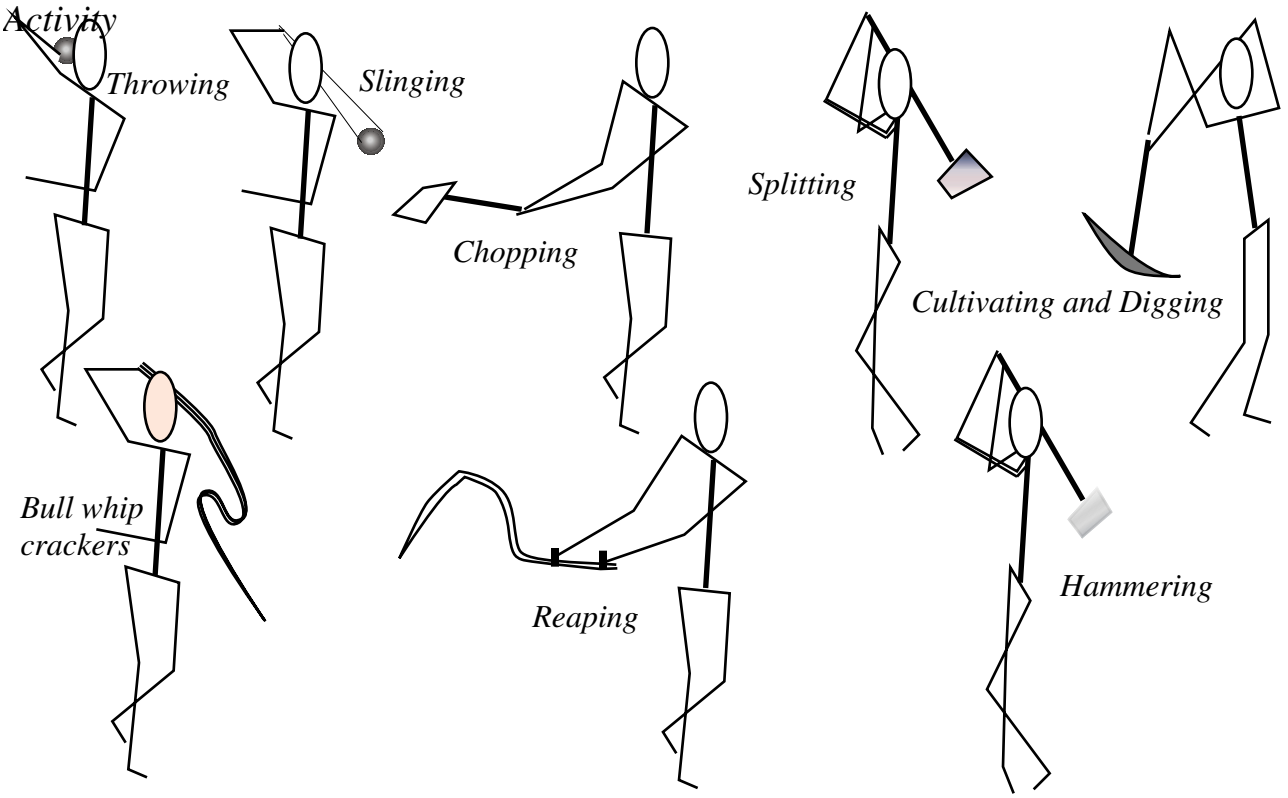

(b) Later Human Recreational Activity

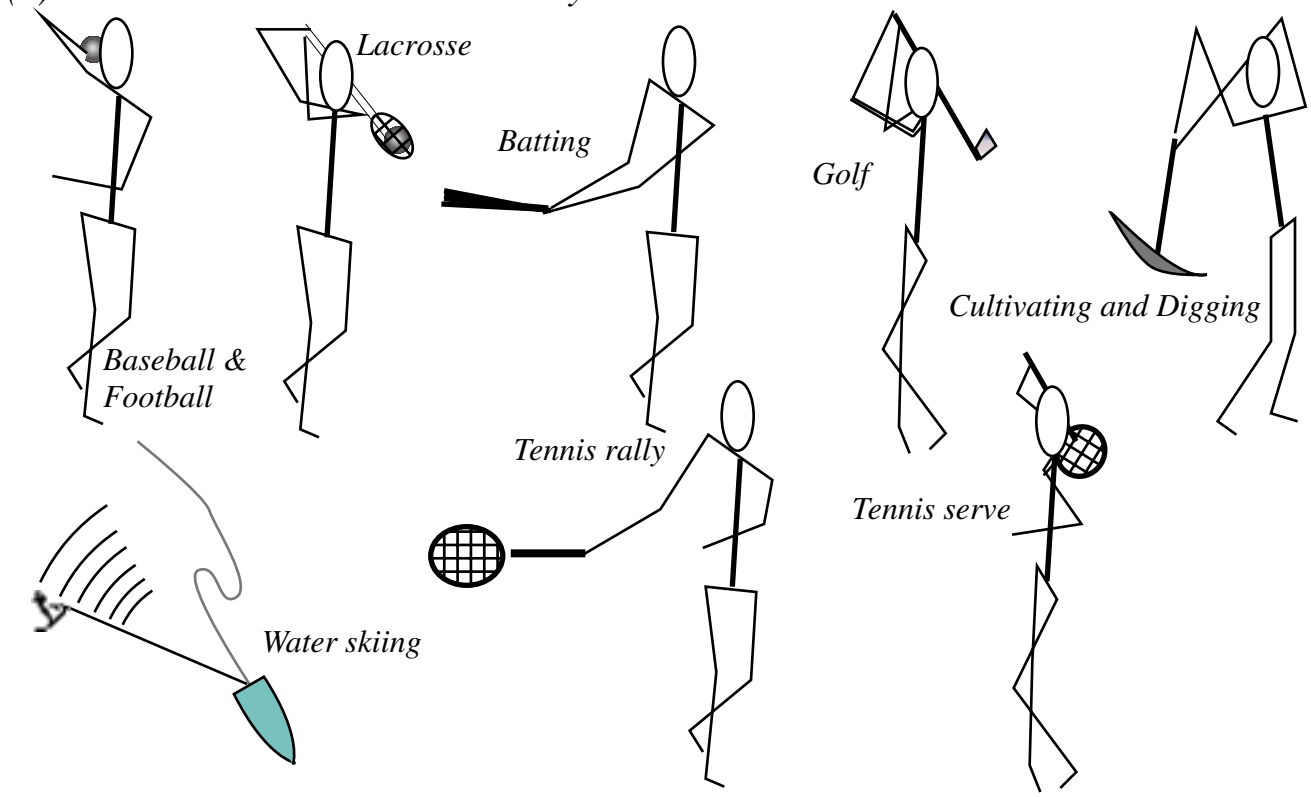

Fig. 2 (c) Human motions are approximated by the trebuchet.

These have been executed billions of times to bring human history and culture to the point where it is now. It was the motion of the scythe that reaped our ancestors grain, the swing of the ax that cleared our forests, the arc of the pick that quarried and dug for our buildings, the muscle and hammer that pounded our rail spikes. All the motions in Fig. 2(c) are related to the non-linear dynamics of the trebuchet. Add to this lassoes, whips, and sling-shots. Analytical difficulty is no excuse to ignore such a problem!

Nowadays machines do most of our chopping, digging, cultivating, and reaping. Strangely, however, it seems that this has made this particular physics problem even more acutely relevant. In a leisure culture, humans seem unable to stop their chopping, digging, cultivating, and reaping motions, as they become fascinated with a multitude of sports including baseball, golf, tennis, or racquetball that mimic these motions. We pay millions in pursuit of a perfect stroke or swing. Should not physicists have something helpful to say about some of the most overwhelming human obsessions? If a physics instructor can tell a student how to ring the bell at a county fair by analyzing trebuchets, this may be the most appreciated idea in the course.

Such is the motivation for devoting a large part of a required mechanics with C++ programming course to the thousand year old trebuchet dynamics [5]. Also, as explained later, it is an excellent problem to introduce the use of generalized coordinates and Lagrangian-Hamiltonian formulations. It is non-trivial and full of wonderful surprises and analogies, while it can also be simplified by taking special cases such as the simple pendulum in Fig. 2 to introduce or review basic ideas. But the overriding motivation is its incredible connections with human behavior as well as with various areas of physics.

With some thought (and computer simulation) the kinematics and dynamics of the fiendish trebuchet are amenable to qualitative and semi-quantitative approximations which apply to some sports-related biomechanical analogies alluded to above. These analogies will be discussed first below.

3. Qualitative analysis and sports biomechanical analogy

One of the most difficult parts of teaching physics is disabusing students of the Aristotelian misconception that applied force gives immediate and proportional velocity. It also turns out to be one of the most difficult misconceptions to overcome in "lever sports" like tennis, golf, or baseball. Understanding the trebuchet energy transfer may help to dispel such misconceptions.

A simulation of a trebuchet in Fig. 3 shows how and when energy is transferred from the big mass M to the much smaller projectile m. The only power channel to mass m is the tension vector **F** along the rope ℓ. Since power is the scalar product **F•v** of force and velocity **v**, the big lever r_b has to do all its work early on when **F** and **v** are nearly collinear and well before the rope swings out perpendicular to velocity **v**. (Then **F•v** becomes zero or negative.) The later part of the trajectory in Fig. 3b serves only to steer or aim mass m in preparation for delivery.

This may help to explain why an expert 14-year-old can accurately hit *80 mph* tennis drives while a typical adult "hacker" can barely produce or control shots with less than half this speed. The trick is to get energy into m at the lever end (racquet head) early when it is way behind the point where the energy is going to be used. An early force **F** is more effective pulling along the lever arm ℓ (analogous to a nearly rigid arm-

and-racquet handle) as the mass *m* (racquet head) begins to swing out due to centrifugal force as in Fig. 2a. Furthermore, a large force is produced early and automatically by the massive trebuchet (or player body) pulling along the ℓ-lever as the body *M* rotates. Seemingly effortless tennis power comes from the stronger leg and abdominal flexors rotating one's body analogously to gravity rotating the trebuchet main beam and not from shoulder or arm muscles (of which the trebuchet has none at all.) The shoulder joint should be a relaxed and loose hinge, not a hacking power source.

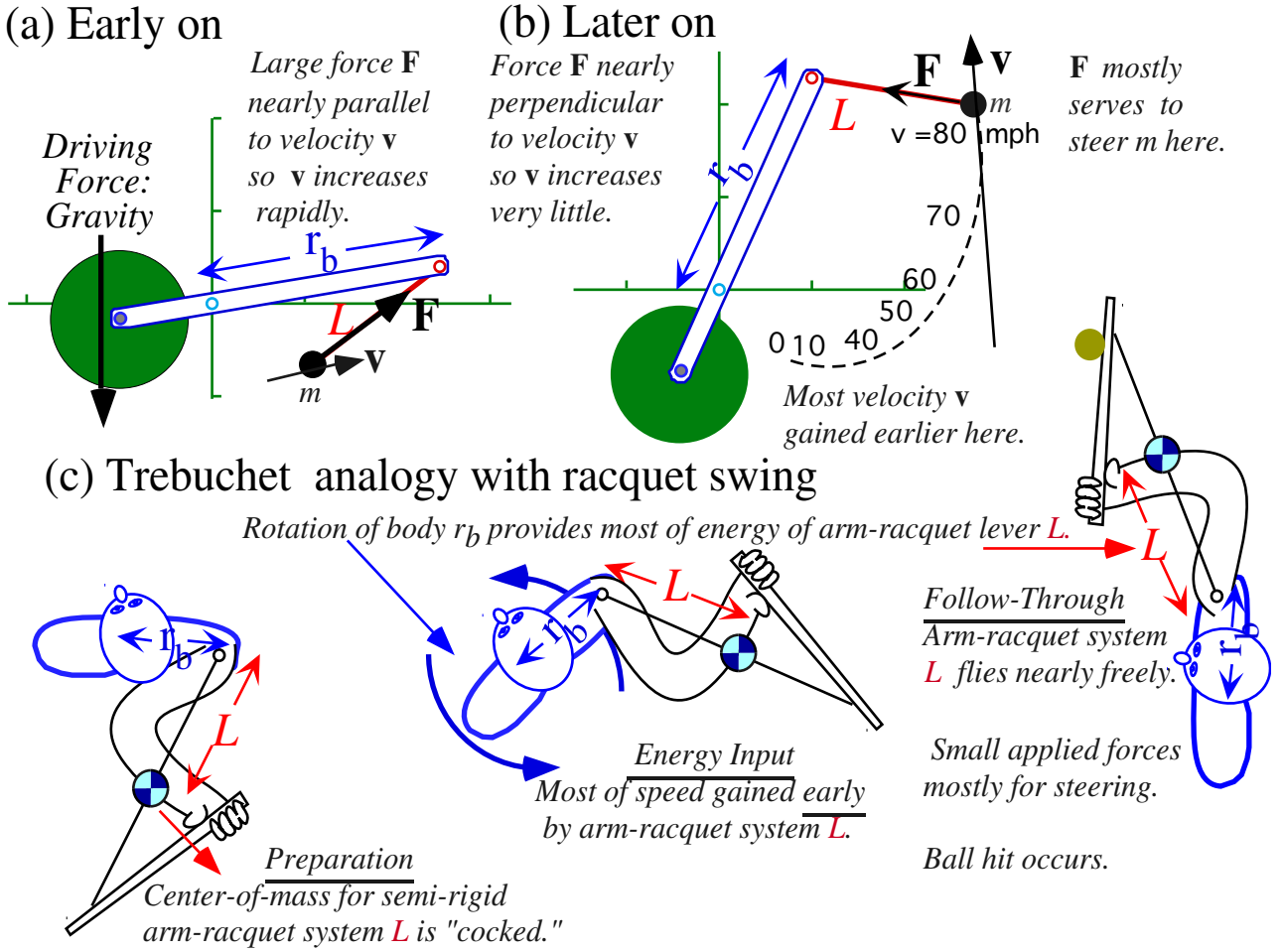

Fig. 3 Example of elementary trebuchet dynamics and qualitative analogy with tennis racquet swing

However, humans can flex and add energy using shoulders or arms. Unfortunately, for a vast majority of unskilled "hackers" in a variety of lever-sports, the tendency to over-use (and damage) ones shoulders, elbows, and wrists is almost unavoidable without proper instruction. The Aristotelian illogic takes over and wrongly demands that the greatest force be applied later in the stroke and particularly at or just before the time of contact. Such a misconception is likely to result in frustration and injury.

A common tennis or golf instructor's mantra is, "Rotate your body!", but it is doubtful that few will (or can) explain physically why. Perhaps, the analogy in Fig. 3c with the trebuchet can help to understand this. Like the trebuchet, expert tennis strokes use the later "follow-through" period to accurately guide and aim a more-or-less rigid arm-racquet system analogous to the trebuchet mass *m* and lever ℓ. In Fig. 3c shoulder

radius is r_b and ℓ is the radius from shoulder to CM of arm-racquet. (ℓ is radius of gyration.) In the follow-through phase, the arm-racquet system, like the trebuchet mass m, has already gained its energy easily and early by r_b rotation pulling along a nearly rigid ℓ . So, the remaining time before ball contact may be devoted to relatively small corrections of flight of ℓ without needing late and ineffectual "hacking" acceleration. Simply put, the shoulder lever or beam r_b smoothly "throws" the arm-racquet system-ℓ at the ball.

Another instructor mantra is, "Let the racquet (or driver) do the work!" Arm muscles should be nearly rigid so as to do little work that helps or hinders the flight. Shoulder muscles should be loose at the shoulder joint like the trebuchet hinge between beam r_b and lever ℓ so as not to hinder (or help) ℓ-speed, either.

In contrast, a "hacker" waiting until the racquet head is approaching the delivery point (Fig. 3b), has to apply a large torque, that is, a large perpendicular force-couple to a lower part of lever ℓ. At this late time a long racquet and arm-lever length ℓ acts to one's disadvantage. Poor leverage reduces the acceleration at the delivery end. (Acceleration of outer end of ℓ is inversely proportional to ℓ.) Also, the racquet-arm system, in a desperate attempt to quickly provide more energy, ceases to be rigid, and degenerates into a complex multi-angle and multi-torque system which has small leverage and is difficult to accurately control. (Between the shoulder and the racquet there are (at least) four independent angles in the wrist and elbow which corresponds to an eight-dimensional phase space that is a human control-system nightmare and a gold-mine for orthopedic surgeons.)

Early application of one's rotating body to pull along the lever ℓ as the trebuchet is doing in Fig. 3a takes advantage of the lever's length ℓ to enhance velocity **v** in the power product **F•v**. (Speed $|\mathbf{v}|$ at outer end of ℓ is directly proportional to product of ℓ with the rate of rotation.) This leaves time for steering the arm-racquet system as it maintains a fairly constant speed during the follow-through period before ball contact, a better situation than having to apply last-minute acceleration that makes racquet attitude and speed vary greatly just before contact. Such "hacking" forces provide less speed and angle control and do more to hurt, wrists, elbows and shoulders than to propel in a controllable way.

4. Semi-quantitative comparison of trebuchet and "flinger"

Consider now a device we will call the "flinger" which seems to (but really doesn't) track one's innate Aristotelian misconceptions about force and velocity. This device is an exact opposite of trebuchet in that it applies most of its force later rather than early and perpendicular rather than along a lever. To use one more sports analogy, this is like a comparison of a pass (flinger launch) to a slap-shot (trebuchet launch) in hockey.

One common way to make a flinger is to insert a pool queue-stick into a lubricated skate-board wheel which may slide down the tapered stick about a half way before being stopped by the thicker handle. Then the pool stick is cast like a fly-fishing rod so that the wheel flies off with enough speed to go quite a distance. (See Fig. 6b in the following section.)

Many of us have, at one time or another, done something like this with an apple pierced by a stick. However, apples tend to stick to a stick more than the skateboard wheel does, and so the apple may also get an appreciable initial longitudinal force just like the trebuchet projectile. The wheel on the flinger, however, slides with negligible friction so it cannot take much advantage of trebuchet-like energy transfer. Rather

flinging relies solely on orthogonal forces and torques which increase as the stick rotates; its physics is quite the opposite to that of the trebuchet. Also, flinging applies force later rather than earlier and requires large (arm wrenching) torque.

A flinger simulation that is set up to be gravity-driven like the trebuchet is shown in Fig. 4. The projectile energies achieved by the flinger are well below those of the trebuchet with similar mass and lever ratios. However, flinger proponents may object that such a gravity driven device unfairly penalizes flinging which, unlike trebucheting, puts off most of its work to the last moment, just when the main beam is slowing down.

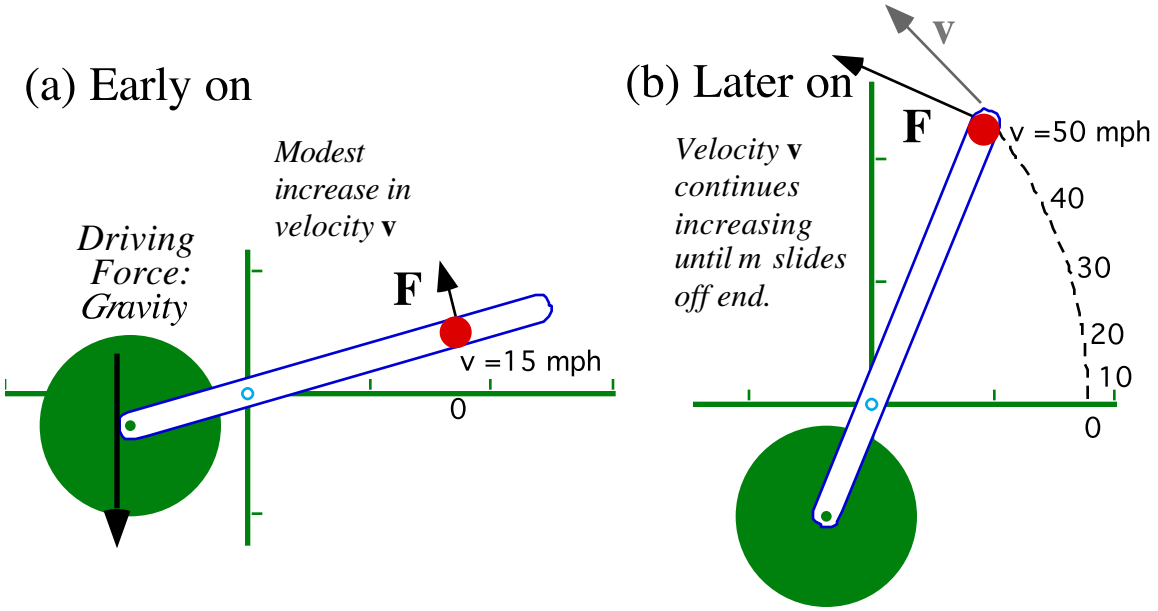

Fig. 4 Example of elementary "flinger" dynamics and qualitative analysis

To address these objections, let us imagine that either system is mounted on a main beam that turns with constant angular velocity ω as sketched in Fig. 5. Also, we will handicap the trebuchet by starting it out in a disadvantageous half-cocked initial position as seen in Fig. 5a. This starting position is more like a *6-o'clock* racquet-back-and-ready position often recommended for tennis. (Initially, the racquet handle butt points at the incoming ball and is drawn like a sword toward it.) Full-cocked *8-9 o'clock* positions used by ancient ingeniators to maximize a trebuchet's range are more appropriate for golf or baseball. These are calculated below, too.

For a mass fixed in a rotating frame at radius r the centrifugal acceleration is $\omega^2 r$ radially outward. If the mass is moving with velocity **v** there is an additional Coriolis acceleration of $\boldsymbol{\omega}\times\mathbf{v}$, but since that is normal to the frictionless constraints of this problem, it can be ignored. Then the rotating frame speed can be calculated using an inverted quadratic effective potential

$$V^{centrifugal}(r) = -\frac{1}{2}m\omega^2 r^2 \qquad (1)$$

such that its gradient is the centrifugal force.

$$-\frac{dV^{centrifugal}}{dr} = m\omega^2 r = F^{centrifugal} \qquad (2)$$

It might seem at first that the flinger should win this comparison since radius *r(t)* for *m* will grow as a hyperbolic *cosh ωt* function, that is, eventually exponentially, while the trebuchet seems limited by its pendulum design. However, the trebuchet is gaining speed at a similar rate, albeit from a starting radius R_1 at the *6-o'clock* position which has less potential, but the trebuchet finally redirects its mass toward the tangential direction so its velocity adds directly to the rotation in the inertial lab frame while the flinger only flings *m* radially along the rotating beam.

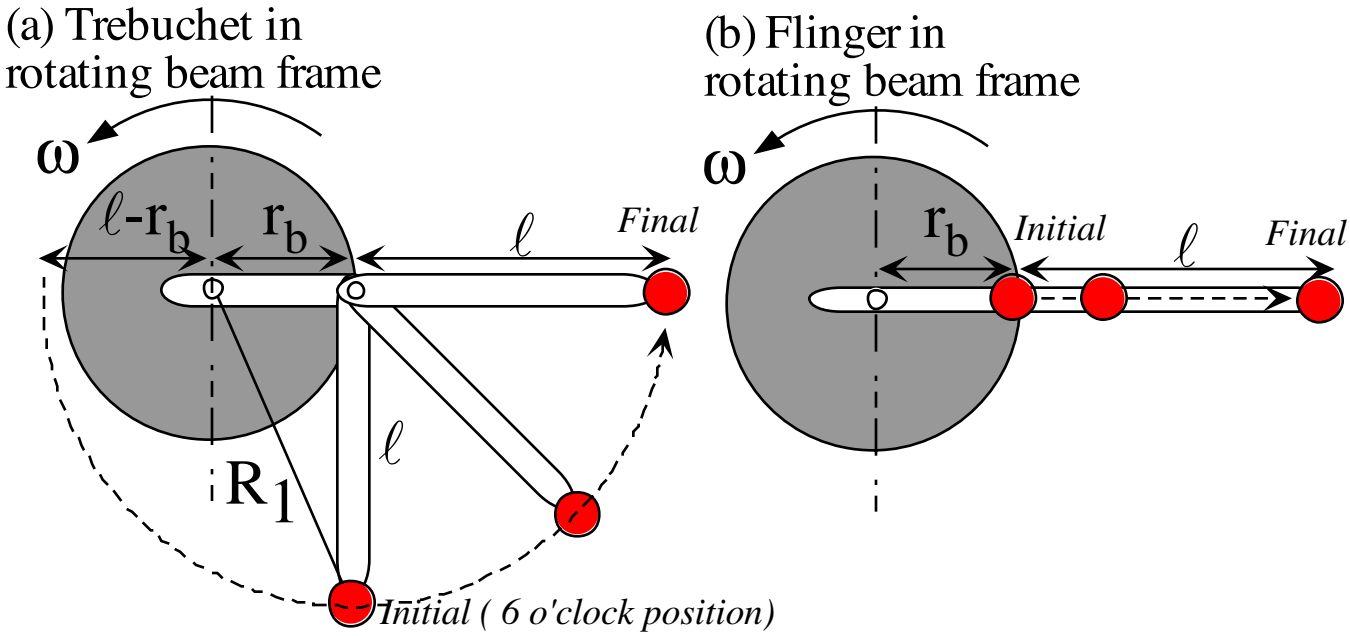

Fig. 5 Comparing rotating frame dynamics of (a) trebuchet and (b) flinger for similar dimensions

Final beam-relative speed $v_{beam\ rel.}$ is found using kinetic energy resulting from a difference of potentials (1) at final radius r_f and initial radius r_0. (Initial beam-relative velocity is assumed zero and gravity is ignored.)

$$\frac{1}{2}mv_{beam\,rel.}^2 = V(r_0) - V(r_f) = \frac{1}{2}m\omega^2 r_f^2 - \frac{1}{2}m\omega^2 r_0^2 \qquad (3)$$

For the flinger the initial radius is $r_0 = r_b$ and the final radius is $r_f = r_b + \ell$.

$$\frac{1}{2}mv_{beam\,rel.}^2(fling.) = \frac{1}{2}m\omega^2(r_b+\ell)^2 - \frac{1}{2}m\omega^2 r_b^2 = \frac{1}{2}m\omega^2\ell(2r_b+\ell) \qquad (4)$$

For the trebuchet the final radius is the same but initial radius is: $r_0 = R_1$ where: $R_1^2 = r_b^2 + \ell^2$ by Fig. 5a

$$\frac{1}{2}mv_{beam\,rel.}^2(treb.) = \frac{1}{2}m\omega^2(r_b+\ell)^2 - \frac{1}{2}m\omega^2(r_b^2+\ell^2) = \frac{1}{2}m\omega^2(2r_b\ell) \qquad (5)$$

The inertial lab-relative final velocity for the flinger is a vector sum of radial velocity $\omega\sqrt{\ell(2r_b+\ell)}$ from (4) and the tangential velocity $\omega(r_b + \ell)$ due to the beam-frame rotation at the end point $r_f = r_b + \ell$.

$$v_{lab\ rel.}(fling.) = \sqrt{v_{beam\,rel.}^2(fling.) + \omega^2(r_b+\ell)^2} = \omega\sqrt{\ell(2r_b+\ell)+(r_b+\ell)^2}$$
$$= \omega\sqrt{2(r_b+\ell)^2 - r_b^2} \qquad (6)$$

The inertial lab-relative final velocity for the trebuchet is a scalar sum of tangential velocity $\omega\sqrt{2\ell r_b}$ from (5) and tangential velocity $\omega(r_b + \ell)$ due to the beam-frame rotation at the end point $r_f = r_b + \ell$.

$$v_{lab\ rel.}(treb.) = \begin{cases} \omega\left(r_b + \ell + \sqrt{2\ell r_b}\right), \textit{ for half - cocked 6 o' clock inital position} \\ \omega\left(r_b + \ell + 2\sqrt{\ell r_b}\right), \textit{ for full - cocked 9 o' clock inital position} \end{cases} \quad (7)$$

The second answer given above is for a fully cocked (*9 o'clock*) trebuchet. It gains by having twice the effective potential drop of a half-cocked (*6 o'clock*) trebuchet, assuming a final release at *3 o'clock*.

We consider numerical comparisons, first with $r_b=2$ and $\ell=1$ (long beam and short lever)

$$v_{lab\ rel.}(treb.) = \begin{cases} 5.00\omega, & half - cocked \\ 5.82\omega, & full - cocked \end{cases} \qquad v_{lab\ rel.}(fling.) = 3.74\omega \quad (8a)$$

then with $r_b=1.5$ and $\ell=1.5$ (medium lever and medium beam)

$$v_{lab\ rel.}(treb.) = \begin{cases} 5.16\omega, & half - cocked \\ 6.00\omega, & full - cocked \end{cases} \qquad v_{lab\ rel.}(fling.) = 3.96\omega \quad (8b)$$

and finally, with $r_b=1$ and $\ell=2$ (short beam and long lever)

$$v_{lab\ rel.}(treb.) = \begin{cases} 5.00\omega, & half - cocked \\ 5.82\omega, & full - cocked \end{cases} \qquad v_{lab\ rel.}(fling.) = 4.12\omega \quad (8c)$$

The flinger starts to catch up with the trebuchet as the lever gets longer, but in the examples above, even a half-cocked trebuchet is clearly superior and is delivering 50% to nearly 100% more energy than a flinger.

Also, it should be noted that this ultra-simplified example of a trebuchet favors equal beam and lever lengths $(r_b=\ell)$, something that is generally borne out in more comprehensive numerical simulations. The flinger, on the other hand just wants a longer and longer lever ℓ which would entail ever greater torques to keep the flinger moving even for a small projectile mass *m*. Some ancient trebuchets threw a four or five ton projectile. It is doubtful that anything could fling such a thing!

The approximate trebuchet analysis ending with equations (7) also provide estimates for biomechanical energy transfer, specifically ancient pick-axing or wood-chopping, later rail spike driving or ringing the bell at the fair. As noted before in the tennis analogy, the secret is to pull as much as possible along the handle using an abdominal powered rotating torso. Shoulder muscle contraction helps, too, but generally should not be wasted applying forces transverse to the lever. Assuming the optimal ratio of torso length r_b and lever ℓ $(r_b=r=\ell)$, the expected final velocity (7) for the hammer head *m* should be approximately $4r\omega$ with energy $8mr^2\omega^2$. For a torso and lever length of $r=2.5$ feet and an average torso rotation rate of $\omega=5$ *radians/second* gives a velocity of *50 feet/s*. For an *8lb* (or *1/4 slug*) hammer head, the kinetic energy is *500 ft.lbs.* which (disregarding friction) sends a *10lb* ringer up to *50 ft*. (Ringers are usually less than *5lbs*, so this is a fairly conservative estimate.)

4. Experiments for comparing trebuchet and flinger

Short of pick-axing or fair-bell-ringing, one may try letting students compete for distance using either a stick and string arrangement that resembles trebuchet mechanics (Fig. 6a) or a flinger arrangement (Fig. 6b). Casting a 1 meter fling stick with a slider *m* starting at 50 centimeters as shown in Fig. 6b provides an easy

comparison to casting a 50 centimeter stick and hook holding a 50 centimeter string-pendulum made from the same mass *m* (a skateboard wheel) as sketched in Fig. 6a. Fig. 6 is a rough attempt at the comparison in Fig. 5.

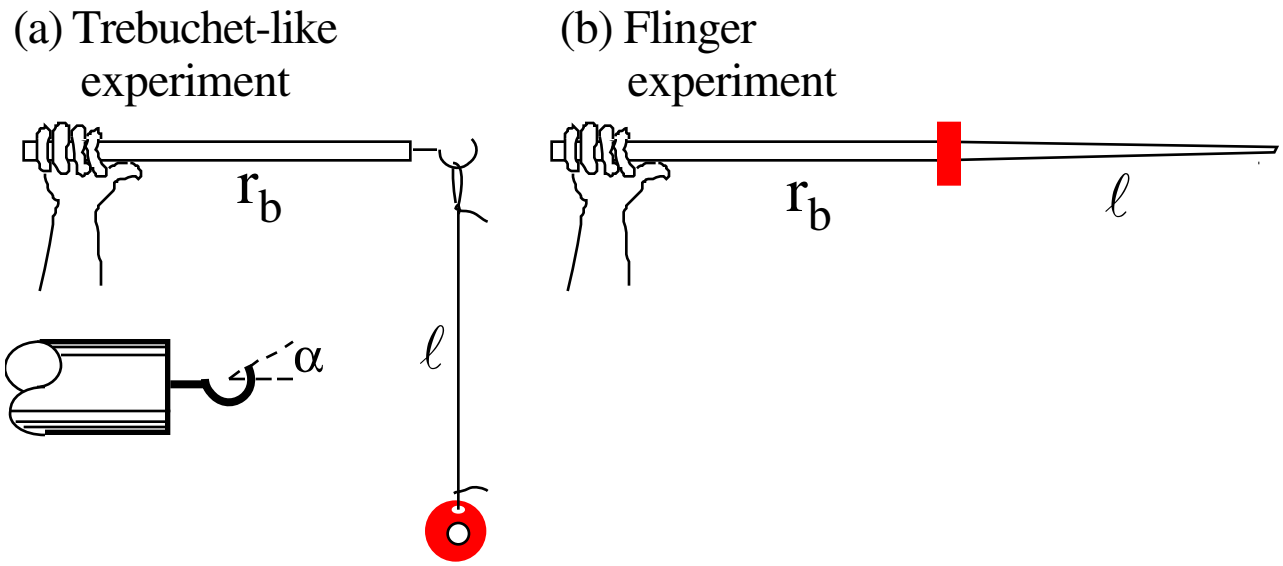

Fig. 6 Simple experiments for comparing dynamics of (a) trebuchet and (b) flinger for similar dimensions.

While good for hours of fun, these experiments can easily degenerate into some pretty sorry science. There are several reasons for this, all interesting in and of themselves, and most penalize the trebuchet model.

First, what is about to happen in Fig. 6 may not correspond to Fig. 5. Students may tend to throw the flinger rather than just rotating it. Since there is some unavoidable longitudinal friction or "stiction" the flinger can gain some of the longitudinal advantage of trebuchet-like acceleration. In any case, it is impossible for either of these sticks to be rotating with a precisely constant angular velocity unless attached to a machine. An initial jerk is necessary to start a launch. A modern video camera and computer is useful for quantifying the actual motion.

Second, humans are natural flingers (like most animals going back to primitive fish). Throwing or any sort of trebuchet-like dynamics requires skill and coaching to be optimal. Students are likely to be more comfortable, at first, with the (Aristotelian) flinger. Unless one does fly-casting or some related activity, the trebuchet model may require some practice and therefore perform less than optimally at first. Learning is an interesting part of this.

Third, the curve and angle α of the release hook on the trebuchet-model stick is fairly critical. As will be shown, $\alpha=0$ gives the optimal range but small variations may be desired for different throwing styles. Release settings are the bane of trebuchets to this day. Failure of Cortez's ingeniators to set the proper release angle resulted in the projectile going straight up and destroying the machine on the first shot! [1] Students who orient the hook sideways or upside down will score an unpleasant hit as the wheel turns on themselves. Caution!

Finally, the string attached to the trebuchet-model skateboard wheel acts as a drag chute and penalizes it accordingly. This should be remedied by making all projectiles identical and attaching strings to the flinger wheels as well. The string can be put through a hole drilled in the plastic wheel so it does not interfere with the sliding action on the flinger stick.

The reproducibility of experiments with hand-held devices sketched in Fig. 6 is dicey, to say the least. However, it does follow somewhat along the lines of the oriental traditions of the inventors of the trebuchet. The Chinese trebuchets were human powered. From ancient drawings we surmise that dozens of tugging men hung on the short end of the beam and pulled with all their might!

Later the Turks began using a big box of rocks instead of tugging men. This improved range and payload as well as reproducibility. For the same reasons, laboratory trebuchets or mounted versions of Fig. 5 or 6 offer a better quantitative experiment, and such devices can be powered by gravity, springs, or even motors with only a little more construction effort beyond that of the hand-held devices. Further, the use of modern technology and materials opens some interesting possibilities for improving such apparatus as the millennial anniversary of the autonomous trebuchet draws nigh. This will be discussed below after introducing other theoretical connections.

5. Relations to ordinary and parametric resonance

There is another universal modern human activity called *twiddling*: swinging one's glasses, keys or a key ring during periods of contemplation or procrastination. Such motion is related to that of the trebuchet and to some other physical phenomena such as quantum waves that might have seemed, at first, totally unrelated.

Suppose you are holding a small mass by a string attached to it as sketched in Fig. 7. This is similar to the trebuchet-model in Fig. 6a if length ℓ could be assumed large compared to the motions.

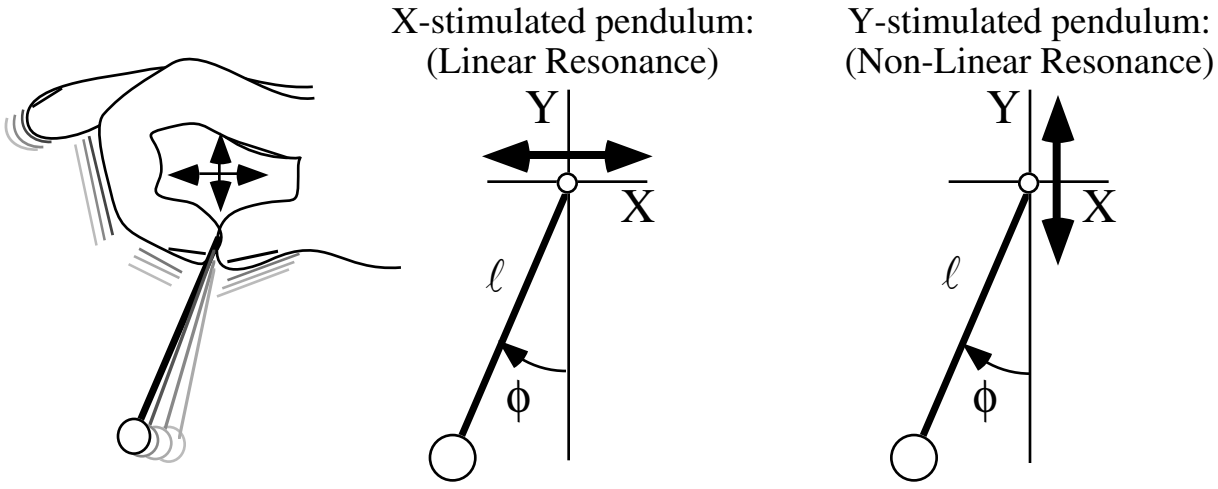

Fig. 7 Two (very different) types of accelerated pendulum resonance .

Wiggling the supporting end of the string may rapidly excite the hanging mass. How rapidly depends on frequency and direction, horizontal *x* or vertical *y*, of the wiggle. Horizontal wiggle would be the most natural for most and leads to ordinary (linear) resonance. However, as shown below, vertical wiggle may cause much more rapid excitation if done correctly and corresponds to *parametric* or *nonlinear* resonance

which is described (for small angles) by an equation that has the same form as the Schrodinger wave equation. [6]

The equations of motion can be derived quite easily by applying the *equivalence principle* to the accelerating frame attached to the pendulum support or hook at the end of a trebuchet beam. According to this, it is only necessary to subtract the acceleration vector **a** of an oscillating frame from the usual vertical gravity acceleration vector **g** to obtain the effective gravity $\mathbf{g}^{eff}$ experienced by the pendulum.

$$\mathbf{g}^{eff} = \mathbf{g} - \mathbf{a}(t) = \begin{pmatrix} 0 \\ -g \end{pmatrix} - \begin{pmatrix} a_x(t) \\ a_y(t) \end{pmatrix} \tag{9}$$

If the support is oscillating in the horizontal direction according to $X_0(t)=A_x\cos(\omega_x t+\alpha_x)$ and in the vertical direction according to $Y_0(t)=A_y\cos(\omega_y t+\alpha_y)$, then the acceleration vector is

$$\mathbf{a}(t) = \begin{pmatrix} a_x(t) \\ a_y(t) \end{pmatrix} = \begin{pmatrix} \ddot{X}^0 \\ \ddot{Y}^0 \end{pmatrix} = \begin{pmatrix} -\omega_x{}^2 A_x \cos(\omega_x t + \alpha_x) \\ -\omega_y{}^2 A_y \cos(\omega_y t + \alpha_y) \end{pmatrix} \tag{10}$$

for arbitrary constant amplitudes A_x, A_y, and phases α_x, and α_y. This gives the following effective gravity vector.

$$\mathbf{g}^{eff}(t) = \begin{pmatrix} g_x^{eff}(t) \\ g_y^{eff}(t) \end{pmatrix} = \begin{pmatrix} \omega_x{}^2 A_x \cos(\omega_x t + \alpha_x) \\ -g + \omega_y{}^2 A_y \cos(\omega_y t + \alpha_y) \end{pmatrix} \tag{11}$$

The general jerked-pendulum equation of motion in such a $\mathbf{g}^{eff}$ field is the following.

$$\frac{d^2\phi}{dt^2} - \frac{g_x^{eff}}{\ell}\cos\phi - \frac{g_y^{eff}}{\ell}\sin\phi = 0 \tag{12}$$

For small angles ($\cos\phi\sim 1$ and $\sin\phi\sim\phi$) this reduces to

$$\frac{d^2\phi}{dt^2} - \frac{g_y^{eff}}{\ell}\phi = \frac{g_x^{eff}}{\ell}. \tag{12a}$$

The two cases indicated in Fig. 7 are *X*-force: $A_x>0$, $A_y=0$ and phase $\alpha_x=\alpha$ or *linear* resonance

$$\frac{d^2\phi}{dt^2} + \frac{g}{\ell}\phi = \frac{\omega_x{}^2 A_x}{\ell}\cos(\omega_x t + \alpha), \tag{12b}$$

or *Y*-force or *parametric* resonance: $A_x=0$, $A_y>0$ with $\alpha_y=\pi$ so $Y(t)$ accelerates upward from a standstill at $t=0$.

$$\frac{d^2\phi}{dt^2} + \left(\frac{g}{\ell} + \frac{\omega_y{}^2 A_y}{\ell}\cos(\omega_y t)\right)\phi = 0 \tag{12c}$$

The *Y*-force equation is a Schrodinger wave equation. (With a cosine potential it is called a *Mathieu equation*.[6])

$$\frac{d^2\phi}{dx^2} + (E - V(x))\phi = 0\ , \quad \text{where: } V(x) = -V_0\cos(nx) \tag{13}$$

Time *t* replaces coordinate *x* as the independent variable, and *y*-effective gravity $-a_y(t)/\ell$ replaces potential $V(x)$.

Equations (12) provide an approximation to trebuchet motion that complements the constant-beam-rotation model sketched in Fig. 5a. The current model has the beam end (supporting pendulum ℓ) initially at rest in a horizontal position and then accelerating upwards to a vertical height of $2A_y=r_b$ according to a simple

harmonic motion function $Y_0(t)=-A_y\cos(\omega_y t)$. Meanwhile, the horizontal position of the pendulum support (also at rest initially) moves left according to $X_0(t)=A_x\cos(\omega_x t)$ with $A_x=r_b$ and $\omega_x=\omega_y/2$. Neither of these exactly track a gravity driven trebuchet beam which would follow a circle and an elliptic time function. (And, this assumes the beam is massive enough to be unaffected by the pendulum ℓ it is throwing.) But, it does provide some insight into the source of the trebuchet's initial accelerative capability.

However, unless ϕ is non-zero and negative, there will be no positive acceleration according to (12c). Non-linear or parametric resonance is not self-starting, quite unlike linear resonance (12b). Angle ϕ of a dead-hanging mass at 6 o'clock is unaffected by a purely vertical acceleration of the support which must rotate to start the centrifugal acceleration. Cocking the pendulum mass toward 7 o'clock or so helps, too, as discussed below. The simple constant-velocity model sketched in Fig. 5a already is rotating relative to the lab frame.

Then the ϕ-acceleration is approximated by

$$\ddot{\phi} = \phi(t)(g+\omega_y{}^2 A_y/\ell)\sim\phi(0)\omega_y{}^2/2$$

(with $r_b=\ell$ and neglecting natural gravity g) Acceleration is amplified because the beam rate ω_y is squared, but a high $\ddot{\phi}$ can be maintained only as long as the beam is accelerating its rotation in the same direction. (For a purely vertical acceleration the maximum velocity is $\phi(0)\omega_y/2$ at $\phi(t)=0$ (6 o'clock), and it would just as rapidly de-accelerate relative to the beam as soon as $\phi(t)$ passed zero.)

6. Trebuchet with constant beam acceleration

Rather than modeling a constant beam angular velocity as in Fig. 5a, we now consider a beam that has constant acceleration. This helps to study any "whip action" that might occur if the beam was accelerated when the lever ℓ is around the perpendicular 6 o'clock position shown in Fig. 6a. We replace the beam coordinate θ with a right-elevation angle θ_B of the beam tip (hook) above horizontal positive X-axis as shown in Fig. 8a .

$$\theta_B = \theta + \pi/2 \qquad (14)$$

Fig. 8a shows a trebuchet in a state for which all coordinate angles and their time derivatives are positive, that is, in counter-clockwise rotation. This means, of course, that the trebuchet is intending to throw to the left. The trebuchet ℓ-lever (or rope) hook will have the following Cartesian lab position relative to the beam pivot.

$$x_{hook} = r_b \cos\theta_B \ , \qquad y_{hook} = r_b \sin\theta_B \ , \qquad (15)$$

The following velocity and acceleration of the hook-relative frame results.

$$\dot{x}_{hook} = -r_b \sin\theta_B \dot{\theta}_B \ , \qquad \dot{y}_{hook} = r_b \cos\theta_B \dot{\theta}_B \qquad (16)$$

$$\ddot{x}_{hook} = -r_b \sin\theta_B \ddot{\theta}_B - r_b \cos\theta_B \dot{\theta}_B{}^2 \ , \qquad \ddot{y}_{hook} = r_b \cos\theta_B \ddot{\theta}_B - r_b \sin\theta_B \dot{\theta}_B{}^2 \qquad (17)$$

We assume a constant beam angular acceleration α beginning at $\theta_B=0$ with initial angular velocity ω_0.

$$\alpha = \ddot{\theta}_B = \ddot{\theta}_B(0), \quad \omega = \dot{\theta}_B = \alpha t + \omega_0, \qquad (18)$$

The equation (12) for lab-relative lever angle ϕ becomes

$$\frac{d^2\phi}{dt^2} = -\frac{\ddot{x}_{hook}}{\ell}\cos\phi - \frac{\ddot{y}_{hook}+g}{\ell}\sin\phi$$
$$= \frac{r_b\ddot{\theta}_B}{\ell}\left(\sin\ \theta_B\cos\phi - \cos\ \theta_B\sin\phi\right) + \frac{r_b\dot{\theta}_B^{\,2}}{\ell}\left(\cos\ \theta_B\cos\phi + \sin\ \theta_B\sin\phi\right) - \frac{g}{\ell}\sin\phi \qquad (19)$$
$$= \frac{r_b}{\ell}\left[\dot{\theta}_B^{\,2}\cos\ (\phi-\theta_B) - \ddot{\theta}_B\sin\ (\phi-\theta_B)\right] - \frac{g}{\ell}\sin\phi$$

The non-gravitational terms depend on an angle ϕ_B between the ℓ-lever (rope) and a perpendicular line dropped toward the positive X-axis from the beam-tip (or hook) as shown in Fig. 8a.

$$\phi - \theta_B = \phi_B = \phi - \theta - \pi/2 \qquad (20)$$

This perpendicular is the direction of the artificial gravity force due to angular acceleration of the beam-tip.

The first term $(\dot{\theta}_B^2\cos\phi_B)$ in (19) is proportional to beam angular velocity-squared and corresponds to the centrifugal effects treated in the constant-velocity model of Section 3. Acceleration of the ϕ-angle due to centrifugal force is largest when $\cos\phi_B = 1$, that is, when $\phi_B = 0$ and the ℓ-lever is perpendicular to the beam.

The second term $(-\ddot{\theta}_B\sin\phi_B)$ in (19) is proportional to beam angular acceleration $\ddot{\theta}_B$. It gives a positive contribution only when $\sin\phi_B < 0$, that is, when the ℓ-lever is still behind the beam-tip perpendicular. As the ℓ-lever catches up to and passes the moving perpendicular, the coefficient $\sin\phi_B$ of $\ddot{\theta}_B$ goes through zero and becomes positive. Then the $-\ddot{\theta}_B\sin\phi_B$-term decelerates the projectile lever unless the beam acceleration turns off. Trebuchet beam acceleration due to gravity is proportional to $MGR\cos\theta_B$ and does go to zero as the beam reaches vertical. If this happens before ϕ_B goes to zero, then the $-\ddot{\theta}_B\sin\phi_B$-term can only add to ϕ-angular velocity.

The maximum positive contribution of the $-\ddot{\theta}_B\sin\phi_B$-term to acceleration of the ϕ-angle occurs whenever $\sin\phi_B = -1$, that is when $\phi_B = \phi - \theta_B = -\pi/2$ or the ℓ-lever is tucked into a 9 o'clock position relative to the beam as it might be for a maximal-range trebuchet shot. However, this does not represent a maximum acceleration of the m-projectile at the lower end of the ℓ-lever; in fact, m's acceleration is exactly zero at this initial moment since the beam is then only rotating the upper (hooked) end of the rope around the mass. Indeed, if the mass is initially on the beam axle with $\ell = r_b$, then it could remain there forever while ϕ grew indefinitely but the beam-relative angle held constant at the initial $\phi_B = -\pi/2$. The important centrifugal term $\dot{\theta}_B^2\cos\phi_B$ can do nothing while the device is in such a state of gimbal-lock. (The 9 o'clock $(\phi_B = -\pi/2)$ position in Fig. 5a is, in fact, an unstable fixed point so gimbal-lock can occur for that model, as well.)

Large initial beam acceleration $\ddot{\theta}_B$ helps "prime" the device, that is, make $\dot{\theta}_B$ positive and get ϕ_B away from $-\pi/2$ so that the centrifugal term $\dot{\theta}_B^2\cos\phi_B$ can start contributing as soon as possible. It may be why ancient trebuchet illustrations [1] show a slightly shorter lever than beam $(\ell < r_b)$; this helps to jerk the projectile away from the 9 o'clock $(\phi_B = -\pi/2)$ lock position. The gravity term $-(g/\ell)\sin\phi$ in (19) also helps to get ℓ started rotating.

Beam acceleration term $-\ddot{\theta}_B\sin\phi_B$ continues to help while the centrifugal $\dot{\theta}_B^2\cos\phi_B$-term grows, but then dies as the latter reaches its maximum. At this point $(\phi_B = 0)$ it is better to have no beam acceleration at

all. A negative beam acceleration $\left(\ddot{\theta}_B < 0\right)$ might seem desirable for maximizing the effect of the $-\ddot{\theta}_B \sin\phi_B$-term in (19) when $\sin\phi_B$ becomes positive. This would be true only if (a) the centrifugal term was gone, and (b) the ℓ-lever could have compression as well as tension. Neither (a) nor (b) hold for a standard trebuchet.

7. Generalized coordinate and Lagrangian approach to trebuchet

The coordinate angles are a classic example of a non orthogonal *generalized curvilinear coordinate (GCC)* system. To see this we plot the coordinate lines ($q^1=\theta$ =*const.*) and ($q^2=\phi$ =*const.*) in Fig. 8b-c or (ϕ_B=*const.*) in Fig. 8d-e. The curved lines (circles, actually) form a coordinate grid or *manifold* that seems to be wrapped around a toris. Two overlapping manifolds such as Fig. 8b and 8c are needed to fully describe a trebuchet.

The manifold shown in Fig. 8b or d applies when the trebuchet is shaped like a left hand and is pulling to throw its projectile to the left. The manifold shown in Fig. 8c or e applies when the trebuchet is shaped like a right hand and is pulling to throw its projectile to the right. (Or else it is in the "carry-over" stage after throwing to the left.) Either drawing appears to be part of a *toris*. The 3-dimensional appearance is, strictly speaking, an optical illusion; these are just circles drawn by using two parts of what is basically a double drafting compass. But, the illusion contains some topological truth. In fact, the upper drawing can be thought of as the "top" of a toris while the lower drawing shows the "bottom" of the same toris. (The latter is more difficult to see since the eye insists on giving a convex illusion.) Together the two surfaces are a covering surface for the entire trebuchet manifold.

The Cartesian coordinates *(X,Y)* of *M* and *(x,y)* of *m* are related to trebuchet angles in Fig. 1 as follows.

$$X = R\sin\theta\ , \qquad x = -r\sin\theta + \ell\sin\phi \tag{21a}$$

$$Y = -R\cos\theta\ , \qquad y = r\cos\theta - \ell\cos\phi \tag{21b}$$

Hereafter, the beam radius r_b is designated simply by r. Velocity relations follow.

$$\begin{aligned} \dot{X} &= R\cos\theta\,\dot{\theta} + 0, \qquad & \dot{x} &= -r\cos\theta\ \dot{\theta} + \ell\cos\phi\,\dot{\phi}, \\ \dot{Y} &= R\sin\theta\,\dot{\theta} + 0, \qquad & \dot{y} &= -r\sin\theta\ \dot{\theta} + \ell\sin\phi\ \dot{\phi}. \end{aligned} \tag{22}$$

The kinetic energy expression is written in terms of the generalized angular coordinates.

$$T = \frac{1}{2}M\left(\dot{X}^2+\dot{Y}^2\right) + \frac{1}{2}m\left(\dot{x}^2+\dot{y}^2\right)$$

$$T = \frac{1}{2}M\left(\left(R\cos\theta\,\dot{\theta}\right)^2+\left(R\sin\theta\,\dot{\theta}\right)^2\right)+\frac{1}{2}m\left(\left(-r\cos\theta\ \dot{\theta}+\ell\cos\phi\,\dot{\phi}\right)^2+\left(-r\sin\theta\ \dot{\theta}+\ell\sin\phi\ \dot{\phi}\right)^2\right)$$

This is simplified into an expression involving a quadratic form.

$$\begin{aligned} T = \frac{1}{2}\left(MR^2+mr^2\right)\dot{\theta}^2 \ &- \ \frac{1}{2}mr\ell\dot{\theta}\dot{\phi}\cos(\theta-\phi) \\ -\frac{1}{2}mr\ell\dot{\phi}\dot{\theta}\cos(\theta-\phi) \ &+ \ \frac{1}{2}m\ell^2\dot{\phi}^2 \qquad = \frac{1}{2}\begin{pmatrix}\dot{\theta} & \dot{\phi}\end{pmatrix}\begin{pmatrix}\gamma_{\theta,\theta} & \gamma_{\theta,\phi}\\ \gamma_{\phi,\theta} & \gamma_{\phi,\phi}\end{pmatrix}\begin{pmatrix}\dot{\theta}\\ \dot{\phi}\end{pmatrix} \end{aligned} \tag{23a}$$

Here the toroidal *kinetic metric coefficient* matrix holds the kinetic coefficients of $\dot{\theta}\dot{\theta}, \dot{\theta}\dot{\phi}, \dot{\phi}\dot{\theta}$, and $\dot{\phi}\dot{\phi}$. in turn.

$$\begin{pmatrix}\gamma_{\theta,\theta} & \gamma_{\theta,\phi}\\ \gamma_{\phi,\theta} & \gamma_{\phi,\phi}\end{pmatrix} = \begin{pmatrix} MR^2+mr^2 & -mr\ell\cos(\theta-\phi)\\ -mr\ell\cos(\theta-\phi) & m\ell^2\end{pmatrix} \tag{23b}$$

The off-diagonal cross-term coefficients ($\gamma_{\theta,\phi} = mr\ell\cos(\theta-\phi) = \gamma_{\phi,\theta}$) are zero if the coordinate lines in Fig. 8 happen to intersect at right angles or *orthogonally*. They do this wherever the ℓ-lever is perpendicular to the main beam or θ–ϕ = ±*90*°. Elsewhere ϕ and θ curves are *affine* or *non* orthogonal.

The gravitational potential has a simple form of *(mass)·(gravity)·(height)* for each mass.

$$V(X, Y, x, y) = MgY + mgy \tag{24}$$

The total Lagrangian *L = T - V* satisfies *Lagrange's potential equations*

$$\dot{p}_\theta = \frac{d}{dt}\left(\frac{\partial L}{\partial \dot{\theta}}\right) = \frac{\partial L}{\partial \theta} \qquad \dot{p}_\phi = \frac{d}{dt}\left(\frac{\partial L}{\partial \dot{\phi}}\right) = \frac{\partial L}{\partial \phi} \tag{25}$$

where the p_ϕ and p_θ are the canonical momenta conjugate to coordinates ϕ and θ respectively.

The momentum p_θ conjugate to coordinate θ is given.

$$\begin{aligned} p_\theta &= \frac{\partial T}{\partial \dot{\theta}} = \frac{\partial}{\partial \dot{\theta}}\left(\frac{1}{2}\left(MR^2 + mr^2\right)\dot{\theta}^2 + \frac{1}{2}m\ell^2\dot{\phi}^2 - mr\ell\dot{\theta}\dot{\phi}\cos(\theta-\phi)\right) \\ &= \left(MR^2 + mr^2\right)\dot{\theta} - mr\ell\dot{\phi}\cos(\theta-\phi) \end{aligned} \tag{26a}$$

The momentum p_ϕ is conjugate to coordinate ϕ is as follows.

$$\begin{aligned} p_\phi &= \frac{\partial T}{\partial \dot{\phi}} = \frac{\partial}{\partial \dot{\phi}}\left(\frac{1}{2}\left(MR^2 + mr^2\right)\dot{\theta}^2 + \frac{1}{2}m\ell^2\dot{\phi}^2 - mr\ell\dot{\theta}\dot{\phi}\cos(\theta-\phi)\right) \\ &= m\ell^2\dot{\phi} - mr\ell\dot{\theta}\cos(\theta-\phi) \end{aligned} \tag{26b}$$

It is important to note that the generalized momenta (p_θ , p_ϕ) in (26) are related to the generalized velocities ($\dot{\theta}, \dot{\phi}$) through what were called kinetic metric tensor coefficients ($\gamma_{\mu,\nu}$) in (23).

$$p_\mu = \Sigma\gamma_{\mu\nu}\ \dot{\nu}, \text{ or } \begin{pmatrix} p_\theta \\ p_\phi \end{pmatrix} = \begin{pmatrix} \gamma_{\theta,\theta} & \gamma_{\theta,\phi} \\ \gamma_{\phi,\theta} & \gamma_{\phi,\phi} \end{pmatrix}\begin{pmatrix} \dot{\theta} \\ \dot{\phi} \end{pmatrix} = \begin{pmatrix} MR^2 + mr^2 & -mr\ell\cos(\theta-\phi) \\ -mr\ell\cos(\theta-\phi) & m\ell^2 \end{pmatrix}\begin{pmatrix} \dot{\theta} \\ \dot{\phi} \end{pmatrix} \tag{27}$$

The left side of the Lagrange equations (25) are the following momentum.

$$\begin{aligned} \dot{p}_\theta = \frac{d}{dt}p_\theta &= \frac{d}{dt}\left(\left(MR^2 + mr^2\right)\dot{\theta} - mr\ell\dot{\phi}\cos(\theta-\phi)\right) \\ &= \left(MR^2 + mr^2\right)\ddot{\theta} - mr\ell\ddot{\phi}\cos(\theta-\phi) + mr\ell\dot{\phi}(\dot{\theta}-\dot{\phi})\sin(\theta-\phi) \\ &= \left(MR^2 + mr^2\right)\ddot{\theta} - mr\ell\ddot{\phi}\cos(\theta-\phi) + mr\ell\dot{\theta}\dot{\phi}\sin(\theta-\phi) - mr\ell\dot{\phi}^2\sin(\theta-\phi) \end{aligned} \tag{28a}$$

$$\begin{aligned} \dot{p}_\phi = \frac{d}{dt}p_\phi &= \frac{d}{dt}\left(m\ell^2\dot{\phi} - mr\ell\dot{\theta}\cos(\theta-\phi)\right) \\ &= m\ell^2\ddot{\phi} - mr\ell\ddot{\theta}\cos(\theta-\phi) + mr\ell\dot{\theta}(\dot{\theta}-\dot{\phi})\sin(\theta-\phi) \\ &= m\ell^2\ddot{\phi} - mr\ell\ddot{\theta}\cos(\theta-\phi) + mr\ell\dot{\theta}^2\sin(\theta-\phi) - mr\ell\dot{\theta}\dot{\phi}\sin(\theta-\phi) \end{aligned} \tag{28b}$$

Lagrange equations (25) relate momentum derivatives $\dot{p}_\theta$ and $\dot{p}_\phi$ to generalized forces F_θ and F_ϕ.

$$\begin{aligned} \dot{p}_\theta - \frac{\partial L}{\partial \theta} &= F_\theta = -MgR\sin\theta + mgr\sin\theta \\ \dot{p}_\phi - \frac{\partial L}{\partial \phi} &= F_\phi = -mg\ell\ \sin\phi \end{aligned} \tag{29}$$

$$\begin{aligned} -MgR\sin\theta + mgr\sin\theta &= \left(MR^2 + mr^2\right)\ddot{\theta} - mr\ell\ddot{\phi}\cos(\theta-\phi) - mr\ell\dot{\phi}^2\sin(\theta-\phi) \\ -mg\ell\sin\phi &= m\ell^2\ddot{\phi} - mr\ell\ddot{\theta}\cos(\theta-\phi) + mr\ell\dot{\theta}^2\sin(\theta-\phi) \end{aligned} \tag{30}$$

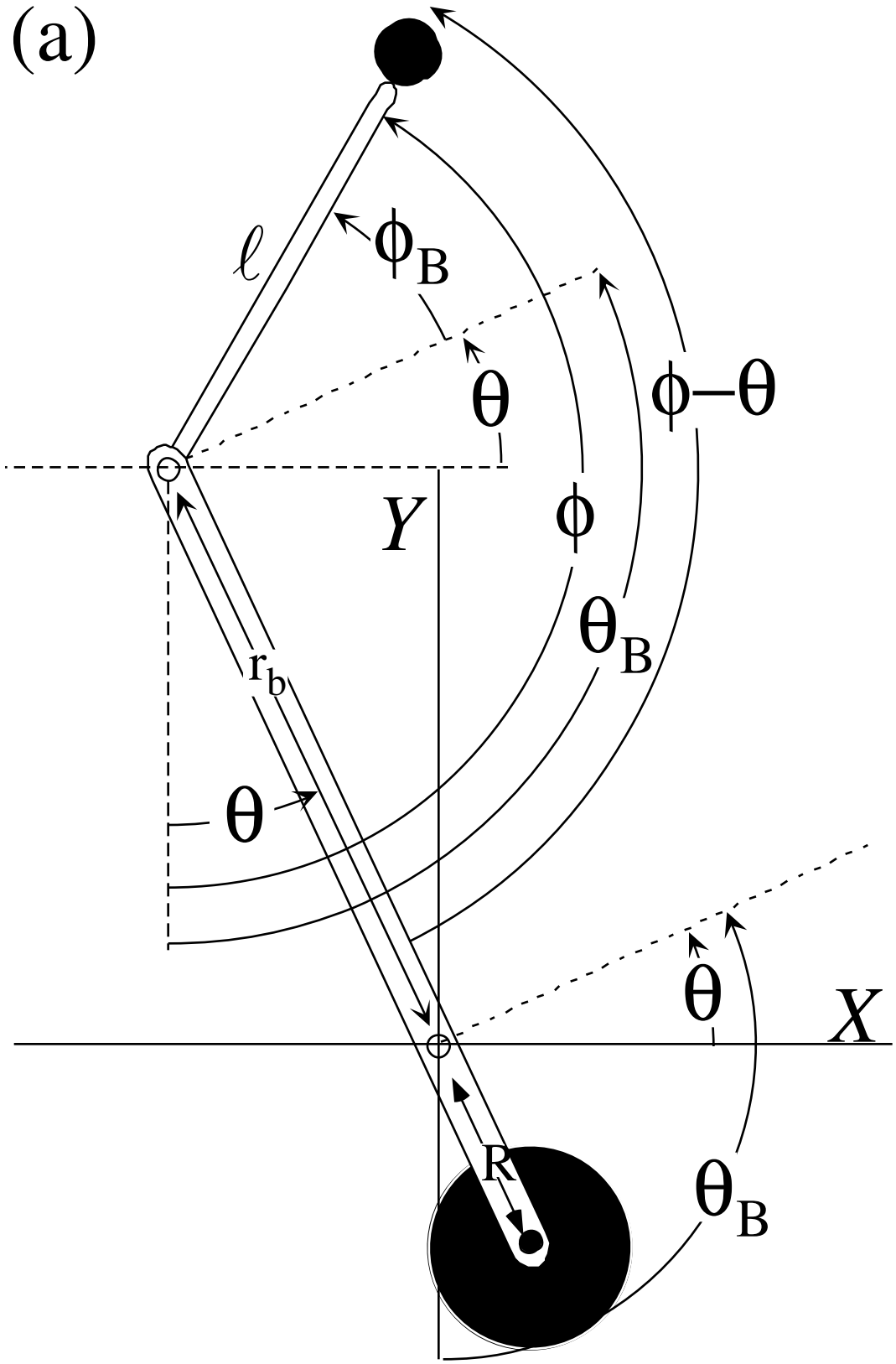

Fig. 8 Trebuchet Coordinates
(a) Glossary of possible coordinate angles for trebuchet (All values shown are positive.)

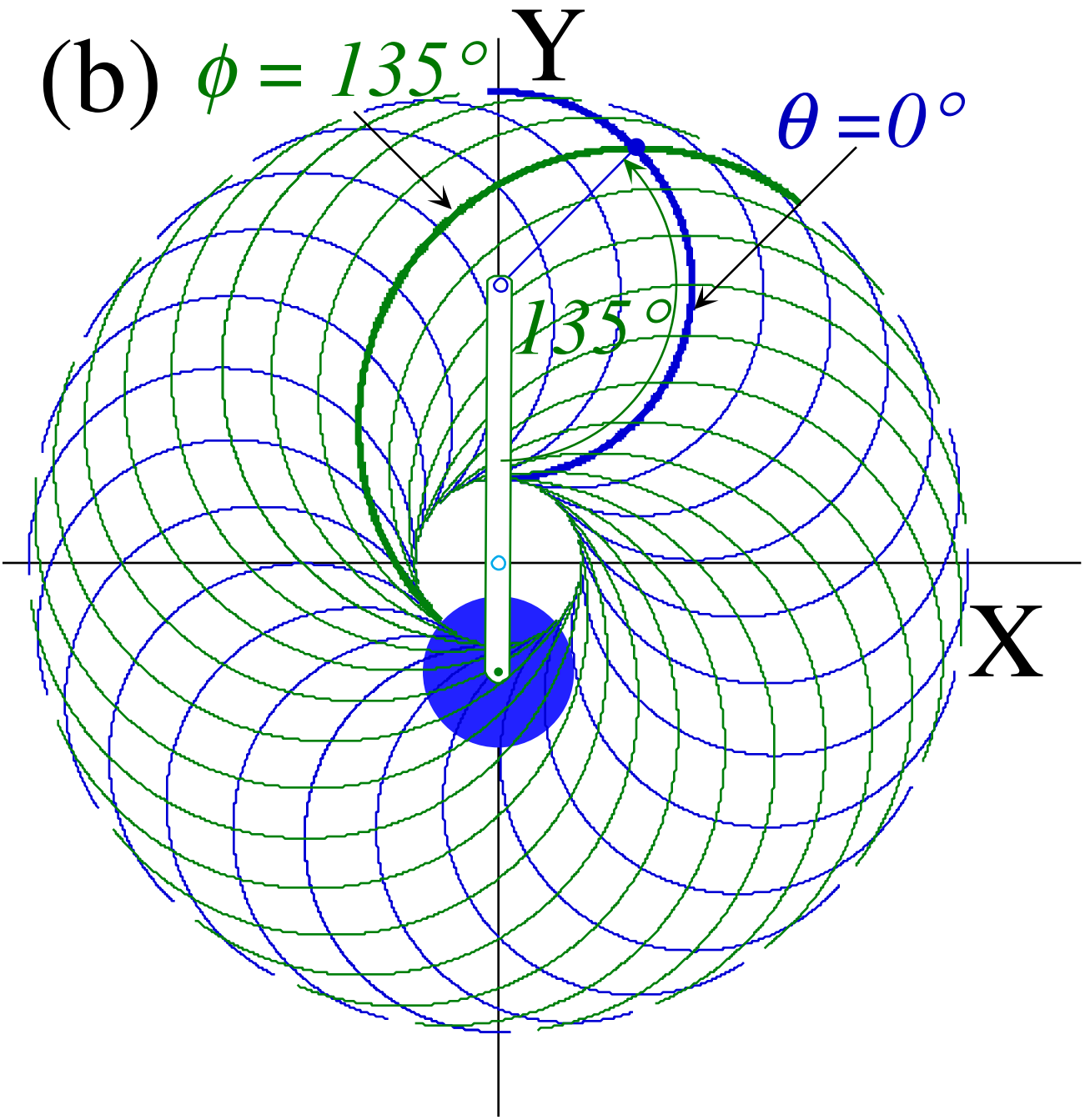

Fig. 8 Trebuchet Coordinates (b) Left-handed (θ,ϕ)-manifold hilighting θ=0 and ϕ=3π/4 lines.

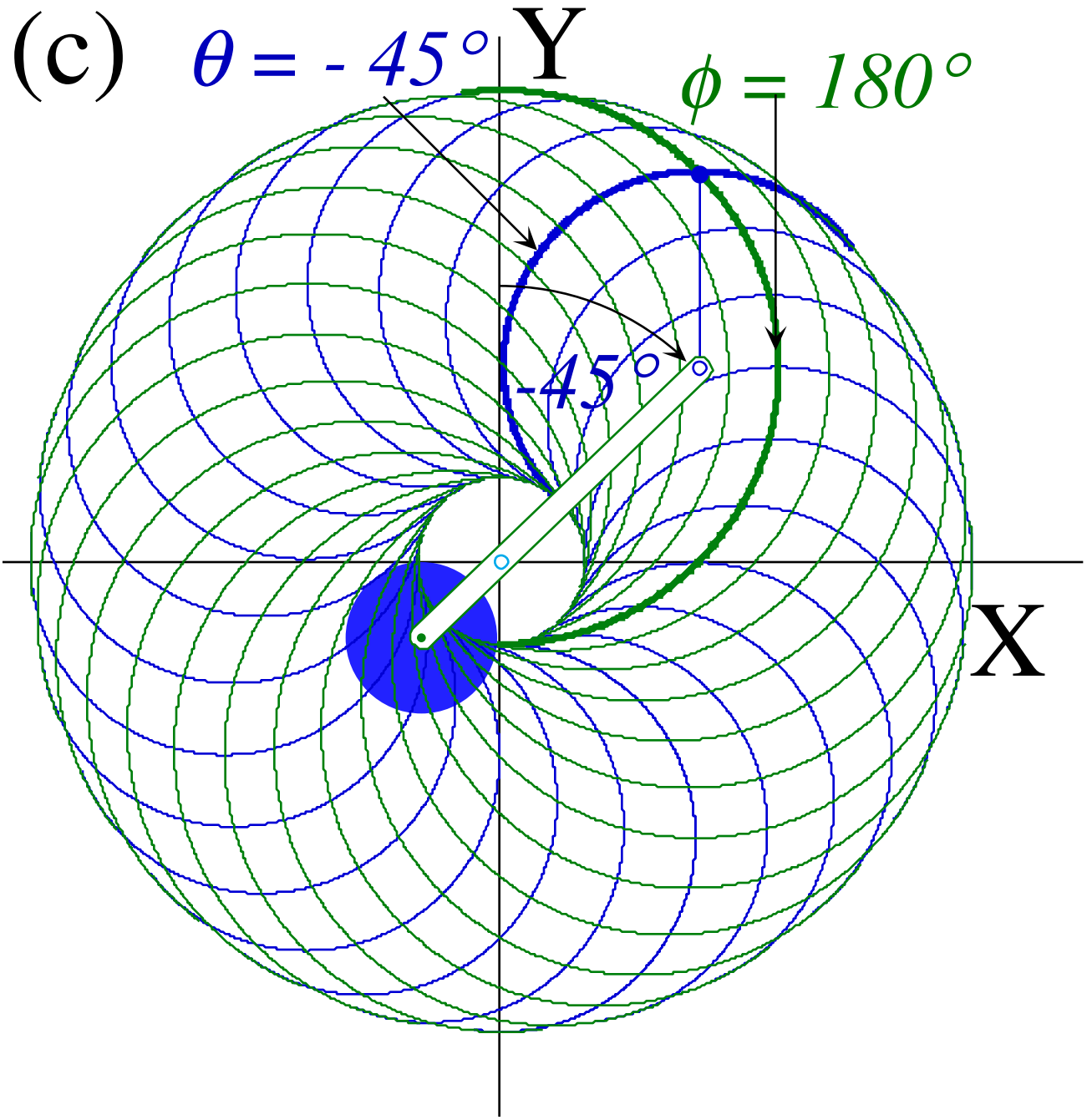

Fig. 8 Trebuchet Coordinates (c) Right-handed (θ,ϕ)-manifold hilighting θ=–π/4 and ϕ=π lines

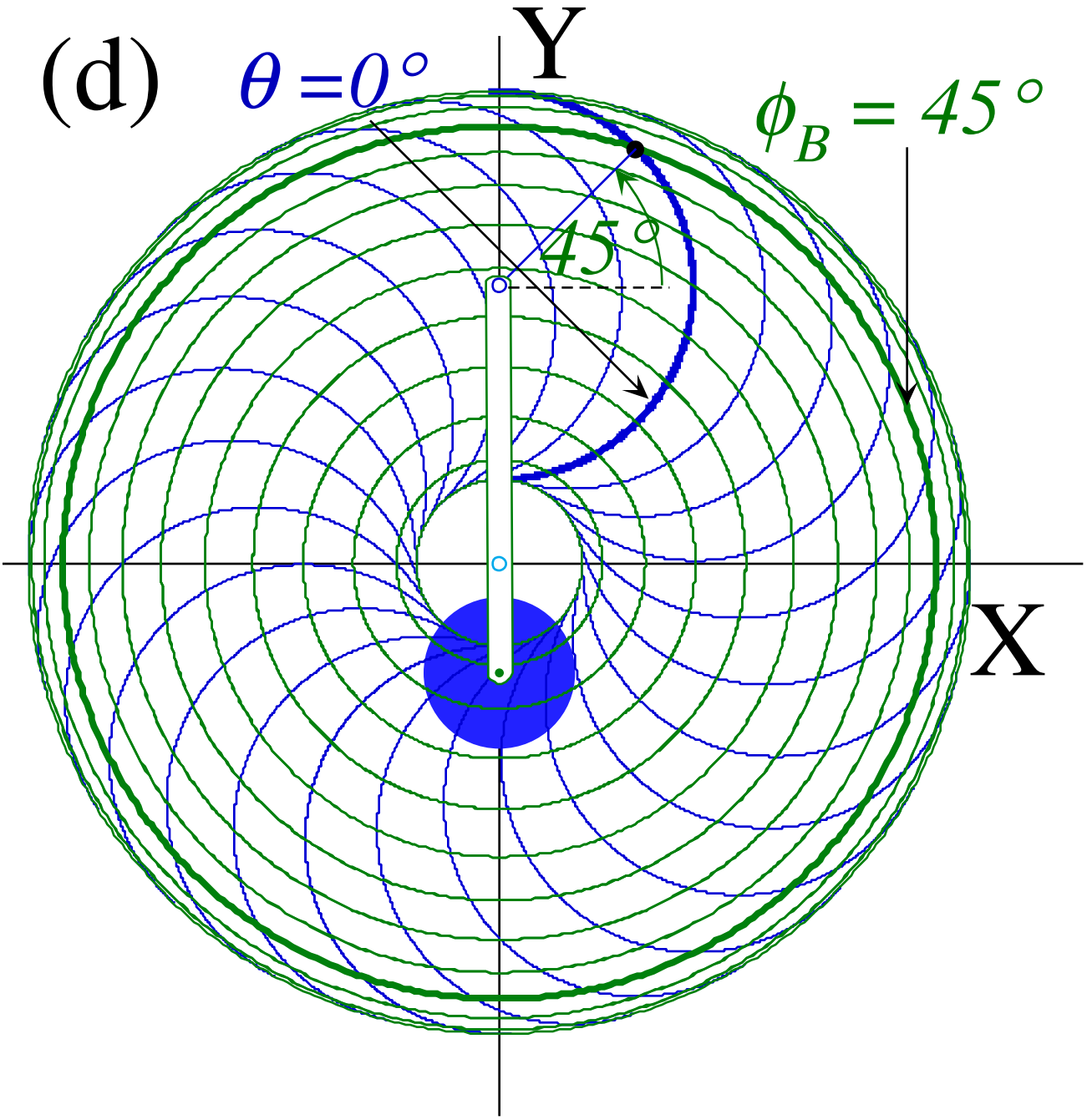

Fig. 8 Trebuchet Coordinates (d) Left-handed (θ,ϕ_B)-manifold hilighting θ=0 and ϕ_B=π/4 lines

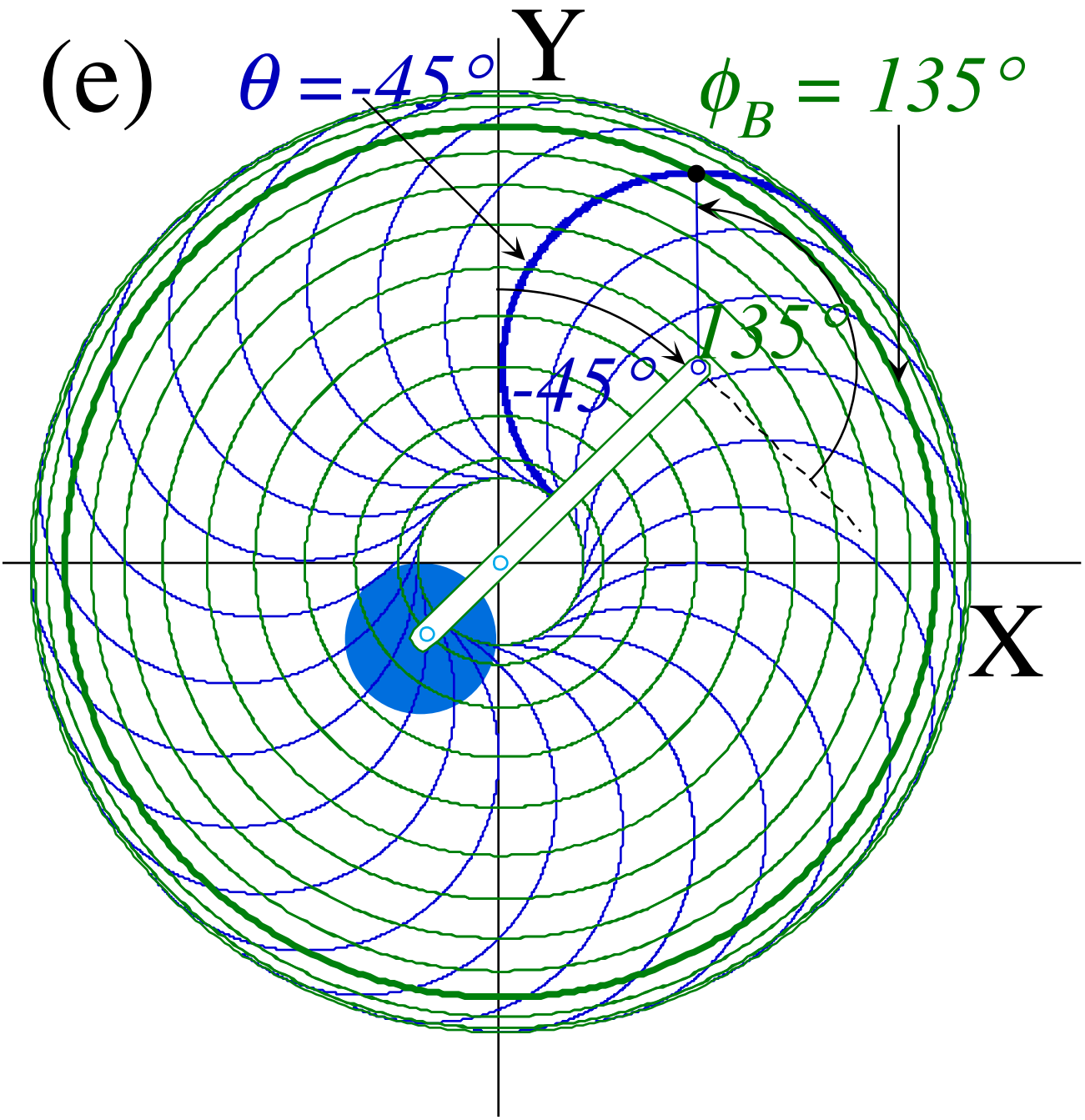

Fig. 8 Trebuchet Coordinates (e) Right-handed (θ,ϕ_B)-manifold hilighting θ=–π/4 and ϕ_B=3π/4 lines

8. Riemann-Christoffel equations: Numerical solution

Lagrangian equations of complex systems are often not in a form that is readily amenable to approximate or numerical solution. Numerical solution favors explicit expressions for the highest derivatives of the dependent variables. We rewrite the equations (30) in matrix form in order to highlight the metric coefficient matrix (23) and give a form that readily allows solving for the highest derivatives.

$$\begin{pmatrix}(mr-MR)g\sin\theta\\ -mg\ell\sin\phi\end{pmatrix}=\begin{pmatrix}MR^2+mr^2 & -mr\ell\cos(\theta-\phi)\\ -mr\ell\cos(\theta-\phi) & m\ell^2\end{pmatrix}\begin{pmatrix}\ddot\theta\\ \ddot\phi\end{pmatrix}+\begin{pmatrix}-mr\ell\dot\phi^2\\ mr\ell\dot\theta^2\end{pmatrix}\sin(\theta-\phi) \tag{31}$$

By inverting the metric matrix we get an equation with the highest derivatives given explicitly.

$$\begin{aligned}\begin{bmatrix}\ddot\theta\\ \ddot\phi\end{bmatrix}&=\frac{1}{\mu}\begin{pmatrix}m\ell^2 & mr\ell\cos(\theta-\phi)\\ mr\ell\cos(\theta-\phi) & MR^2+mr^2\end{pmatrix}\left[\begin{pmatrix}mr\ell\dot\phi^2\\ -mr\ell\dot\theta^2\end{pmatrix}\sin(\theta-\phi)+\begin{pmatrix}(mr-MR)g\sin\theta\\ -mg\ell\sin\phi\end{pmatrix}\right]\\ &=\frac{1}{\mu}\begin{pmatrix}m\ell^2 & mr\ell\cos(\theta-\phi)\\ mr\ell\cos(\theta-\phi) & MR^2+mr^2\end{pmatrix}\begin{bmatrix}mr\ell\dot\phi^2\sin(\theta-\phi)+(mr-MR)g\sin\theta\\ -mr\ell\dot\theta^2\sin(\theta-\phi)-mg\ell\sin\phi\end{bmatrix}\end{aligned} \tag{32}$$

$$\text{where: }\ \mu=m\ell^2\left[MR^2+mr^2-mr^2\cos^2(\theta-\phi)\right]=m\ell^2\left[MR^2+mr^2\sin^2(\theta-\phi)\right]$$

The metric determinant μ is non-zero even when trebuchet is tucked-in or stretched-out. So the equations are free of singularities for numerical Runga-Kutta integration. (32) is used in the *C++* simulations shown in Figs. 3a-b.

Numerically solvable equations can be found for any general kinetic energy having a metric form

$$T=\sum\nolimits_{mass\,a}\frac{m(a)}{2}\dot s^2(a)=\frac{1}{2}\gamma_{m\,n}\dot q^m\dot q^n, \tag{33}$$

as in (23a). Kinetic $\gamma_{\mu\nu}$ are metric coefficients $g_{\mu\nu}$ with mass included. The inhomogeneous Lagrange equations

$$F_\ell=\frac{d}{dt}\frac{\partial T}{\partial\dot q^\ell}-\frac{\partial T}{\partial q^\ell}, \tag{34}$$

expose the components F_m of generalized force which are given here in terms of Cartesian f_j .

$$F_m=f_j\frac{\partial x^j}{\partial q^m} \tag{35}$$

Lagrange equations may be written as *covariant Riemann-Christoffel equations* (of which (31) is an example)

$$F_\ell=\gamma_{\ell n}\ddot q^n+\Gamma_{mn;\ell}\dot q^m\dot q^n, \tag{36a}$$

where the *kinetic Christoffel coefficients of the first kind* are defined by

$$\Gamma_{mn;\ell}\equiv\frac{1}{2}\left[\frac{\partial\gamma_{n\ell}}{\partial q^m}+\frac{\partial\gamma_{\ell m}}{\partial q^n}-\frac{\partial\gamma_{mn}}{\partial q^\ell}\right]. \tag{36b}$$

For numerical solutions we use the *contravariant Riemann-Christoffel equations* (of which (32) is an example)

$$F^k=\ddot q^k+\Gamma_{mn}{}^k\dot q^m\dot q^n \tag{37a}$$

where the *kinetic Christoffel coefficients of the second kind* are defined by

$$\Gamma_{mn}{}^k=\gamma^{k\ell}\Gamma_{mn;\ell}, \tag{37b}$$

and the *contravariant generalized force F^k* is, using (35), given in terms of Cartesian f_j.

$$F^k=\gamma^{k\ell}F_\ell=\gamma^{k\ell}\frac{\partial x^j}{\partial q^\ell}f_j, \tag{37c}$$

(37a) holds whether or not generalized force components F_m or Cartesian f_j are expressible as potential gradients.

$$F_m = -\frac{\partial V}{\partial q^m} = f_j \frac{\partial x^j}{\partial q^m} \quad \text{where:} \quad f_j = -\frac{\partial V}{\partial x^j} \quad \text{or:} \quad \mathbf{f} = -\nabla V \tag{37d}$$

The super-indexed metric γ^{kl} in (37) is the inverse of the sub-indexed one which first appeared in (23) and (27).

$$\dot{v} = \Sigma \gamma^{\mu\nu} p_\mu, \text{ or } \begin{pmatrix} \dot{\theta} \\ \dot{\phi} \end{pmatrix} = \begin{pmatrix} \gamma^{\theta,\theta} & \gamma^{\theta,\phi} \\ \gamma^{\phi,\theta} & \gamma^{\phi,\phi} \end{pmatrix} \begin{pmatrix} p_\theta \\ p_\phi \end{pmatrix} = \frac{1}{\mu} \begin{pmatrix} m\ell^2 & mr\ell\cos(\theta-\phi) \\ mr\ell\cos(\theta-\phi) & MR^2+mr^2 \end{pmatrix} \begin{pmatrix} p_\theta \\ p_\phi \end{pmatrix} \tag{37e}$$

Determinant $\mu = \det \gamma_{\mu\nu}$ was given previously. For example, the gravity-free ($g=0$) equation uses $\gamma^{\mu\nu}$.

$$\begin{bmatrix} \ddot{\theta} \\ \ddot{\phi} \end{bmatrix} = \frac{1}{\mu} \begin{pmatrix} m\ell^2 & mr\ell\cos(\theta-\phi) \\ mr\ell\cos(\theta-\phi) & MR^2+mr^2 \end{pmatrix} \begin{bmatrix} mr\ell\dot{\phi}^2 \\ -mr\ell\dot{\theta}^2 \end{bmatrix} \sin(\theta-\phi) \tag{38}$$

Of course, an outer-space trebuchet is an anachronism most absurd. However, (38) is useful for quantifying the horizontal tennis swing in Sec. 2, and for analyzing trebuchet energy transfer when the internal forces dominate the weight of the projectile. This will be discussed using Hamiltonian and Lagrangian mechanics below.

9. Generalized momentum and Hamiltonian approach

A Hamiltonian approach to this problem may not provide numerical advantages over the Lagrangian approach of the preceding section. However, Hamiltonian theory allows for better treatment of symmetry and conservation rules and helps to find optimal generalized coordinate systems and approximate solutions. We introduce an example of this here.

The general Legendre-Poincare' definition of the Hamitonian function in terms of the Lagrangian is

$$H = \sum_{k=1}^{d} p_k \dot{q}^k - L(\dot{q}, q) = H(p, q) \tag{39}$$

For autonomous problems (no explicit time dependence of coordinate definitions or external forces) the Hamiltonian function has a *(KE+PE)* form. The parenthetical equation is numerically (but not formally) correct.

$$H = T + V = \frac{1}{2} \sum_{j=1}^{d} \sum_{k=1}^{d} \gamma^{jk} p_j p_k + V \left(= \frac{1}{2} \sum_{j=1}^{d} \sum_{k=1}^{d} \gamma_{jk} \dot{q}^j \dot{q}^k + V \right) \tag{40a}$$

$$H = \frac{m\ell^2 p_\theta^2 + \left(MR^2 + mr^2\right) p_\phi^2 + 2mr\ell p_\phi p_\theta \cos(\theta-\phi)}{m\ell^2 \left[MR^2 + mr^2 \sin^2(\theta-\phi)\right]} - g(MR - mr)\cos\theta - gm\ell\cos\phi \tag{40b}$$

(Hamiltonians are explicit functions of momenta while Lagrangians are explicit functions of velocity.) The Hamiltonian is a constant of motion according to Hamilton's first equation if there is no explicit t-dependence.

$$\dot{H} = \frac{dH}{dt} = -\frac{\partial L}{\partial t}, \qquad \dot{H} = 0 \text{ and } H = E = const. \text{ if:} \frac{\partial L}{\partial t} = 0 \tag{41}$$

The remaining Hamilton equations for coordinates and momenta determine the trajectory.

$$\dot{p}_j = -\frac{\partial H}{\partial q^j}, \qquad \dot{q}^k = \frac{\partial H}{\partial p^k}. \tag{42}$$

If there is no explicit q^j-dependence for any coordinate q^j, then the momentum p_j conjugate to q^j must also be a constant of motion.

$$\dot{p}_j = 0 \text{ and } p_j = \Lambda = const. \text{ if:} \frac{\partial H}{\partial q^j} = 0 \tag{42}$$

In the absence of gravitational potential $g=0=V$, the trebuchet Hamiltonian is a function only of the beam-relative angle $\phi_B = \phi - \theta - \pi/2$ from (20). A coordinate transformation (Recall Fig.8a) takes advantage of this.

$$\phi_B = \phi - \theta - \pi/2 \quad (43a) \qquad \phi = \phi_B + \theta_B + \pi \quad (43c)$$

$$\theta_B = \theta + \pi/2 \quad (43b) \qquad \theta = \theta_B - \pi/2 \quad (43d)$$

The velocities (for a Lagrangian theory) and momenta (for our Hamiltonian) need to be transformed by Jacobians.

$$\begin{pmatrix} \dot{\theta} \\ \dot{\phi} \end{pmatrix} = \begin{pmatrix} \frac{\partial\theta}{\partial\theta_B} & \frac{\partial\theta}{\partial\phi_B} \\ \frac{\partial\phi}{\partial\theta_B} & \frac{\partial\phi}{\partial\phi_B} \end{pmatrix} \begin{pmatrix} \dot{\theta}_B \\ \dot{\phi}_B \end{pmatrix} = \begin{pmatrix} 1 & 0 \\ 1 & 1 \end{pmatrix} \begin{pmatrix} \dot{\theta}_B \\ \dot{\phi}_B \end{pmatrix}, \quad \begin{pmatrix} \dot{\theta}_B \\ \dot{\phi}_B \end{pmatrix} = \begin{pmatrix} \frac{\partial\theta_B}{\partial\theta} & \frac{\partial\theta_B}{\partial\phi} \\ \frac{\partial\phi_B}{\partial\theta} & \frac{\partial\phi_B}{\partial\phi} \end{pmatrix} \begin{pmatrix} \dot{\theta} \\ \dot{\phi} \end{pmatrix} = \begin{pmatrix} 1 & 0 \\ -1 & 1 \end{pmatrix} \begin{pmatrix} \dot{\theta} \\ \dot{\phi} \end{pmatrix} \tag{44}$$

Transformation of momenta p_k is transpose-inverse to that of $\dot{q}^k$. This maintains the Poincare' invariant (39).

$$\begin{pmatrix} p_\theta^B \\ p_\phi^B \end{pmatrix} = \begin{pmatrix} \frac{\partial\theta}{\partial\theta_B} & \frac{\partial\phi}{\partial\theta_B} \\ \frac{\partial\phi}{\partial\theta_B} & \frac{\partial\phi}{\partial\phi_B} \end{pmatrix} \begin{pmatrix} p_\theta \\ p_\phi \end{pmatrix} = \begin{pmatrix} 1 & 1 \\ 0 & 1 \end{pmatrix} \begin{pmatrix} p_\theta \\ p_\phi \end{pmatrix} \quad (45a) \qquad \begin{pmatrix} p_\theta \\ p_\phi \end{pmatrix} = \begin{pmatrix} \frac{\partial\theta_B}{\partial\theta} & \frac{\partial\phi_B}{\partial\theta} \\ \frac{\partial\theta_B}{\partial\phi} & \frac{\partial\phi_B}{\partial\phi} \end{pmatrix} \begin{pmatrix} p_\theta^B \\ p_\phi^B \end{pmatrix} = \begin{pmatrix} 1 & -1 \\ 0 & 1 \end{pmatrix} \begin{pmatrix} p_\theta^B \\ p_\phi^B \end{pmatrix} \tag{45b}$$

The transformed Hamiltonian is obtained by writing q^k in terms of $q^m{}_B$ using (43c-d) and p_k in terms of $p_m{}^B$ using (45b) and substituting into (40b).

$$H = \frac{m\ell^2\left(p_\theta^B - p_\phi^B\right)^2 + \left(MR^2 + mr^2\right)\left(p_\phi^B\right)^2 - 2mr\ell p_\phi^B\left(p_\theta^B - p_\phi^B\right)\sin\phi_B}{m\ell^2\left[MR^2 + mr^2\cos^2\phi_B\right]} - g(MR - mr)\sin\theta_B - gm\ell\cos(\phi_B + \theta_B) \tag{46}$$

When gravity is zero or negligible, the θ_B-angular momentum is constant ($p_\theta{}^B = \Lambda = const.$) according to (42). This combined with energy conservation (41) gives the following for the *(g=0)* case.

$$H = \frac{m\ell^2\left(\Lambda - p_\phi^B\right)^2 + \left(MR^2 + mr^2\right)\left(p_\phi^B\right)^2 - 2mr\ell p_\phi^B\left(\Lambda - p_\phi^B\right)\sin\phi_B}{m\ell^2\left[MR^2 + mr^2\cos^2\phi_B\right]} = E = const. \tag{47}$$

This is an algebraic quadratic equation relating ϕ_B-angular momentum $p_\phi{}^B$ to angle ϕ_B and constants Λ and E.

$$\left(m\ell^2 + 2mr\ell\sin\phi_B + I\right)\left(p_\phi^B\right)^2 + 2\Lambda\left(mr\ell\sin\phi_B - m\ell^2\right)p_\phi^B = Em\ell^2\left[MR^2 + mr^2\cos^2\phi_B\right] - m\ell^2\Lambda^2 \tag{48a}$$

or

$$\left(1 - 2\frac{r}{\ell}\sin\phi_B + J\right)\left(p_\phi^B\right)^2 + 2\Lambda\left(\frac{r}{\ell}\sin\phi_B - 1\right)p_\phi^B + \Lambda^2 - E\left[I - mr^2\sin^2\phi_B\right] = 0 \tag{48b}$$

The total effective moment of inertia I of the main beam (if m were stuck on the hook end) is defined by

$$I = MR^2 + mr^2 = Jm\ell^2. \tag{48c}$$

10. Coordinate kinetics in gravity-free (g=0) case

If one is seeking kinetic quantities, that is, final velocities, it helps to rewrite conserved momenta $p_\theta{}^B = \Lambda$ and energy *H=E=T (for g=0)* in terms of desired angular velocities $(\dot\theta, \dot\phi)$ using (20), (26) and (45a).

$$\begin{aligned} \Lambda = p_\theta^B &= p_\theta + p_\phi = \left(I\dot\theta + mr\ell\dot\phi\sin\phi_B\right) + \left(m\ell^2\dot\phi + mr\ell\dot\theta\sin\phi_B\right) \\ 2E &= I\dot\theta^2 + 2mr\ell\dot\phi\dot\theta\sin\phi_B + m\ell^2\dot\phi^2 \end{aligned} \tag{49a}$$

For sake of simplicity, we consider the trebuchet for which beam and rope are equal length *(r=ℓ)*.

$$\left.\begin{aligned} \Lambda &= MR^2\dot\theta + mr^2\left(1+\sin\phi_B\right)\left(\dot\theta+\dot\phi\right) \\ 2E &= MR^2\dot\theta^2 + mr^2\left(\dot\theta^2 + 2\dot\phi\dot\theta\sin\phi_B + \dot\phi^2\right) \end{aligned}\right\} \text{(For: } r=\ell) \tag{49b}$$

(49) is found for three relative positions *9 o'clock* (ϕ_B=$-\pi/2$), *6 o'clock* (ϕ_B=0), and *3 o'clock* (ϕ_B=$\pi/2$) shown by Fig. 5 or Fig. 9a-c. Since total angular momentum Λ and energy E remain constant for all three positions, that is, independent of ϕ_B and θ_B, the differing velocities $(\dot\phi_{\pi/2},\dot\theta_{\pi/2})$, $(\dot\phi_0,\dot\theta_0)$, or $(\dot\phi_{-\pi/2},\dot\theta_{-\pi/2})$ at the different positions are easily related to each other.

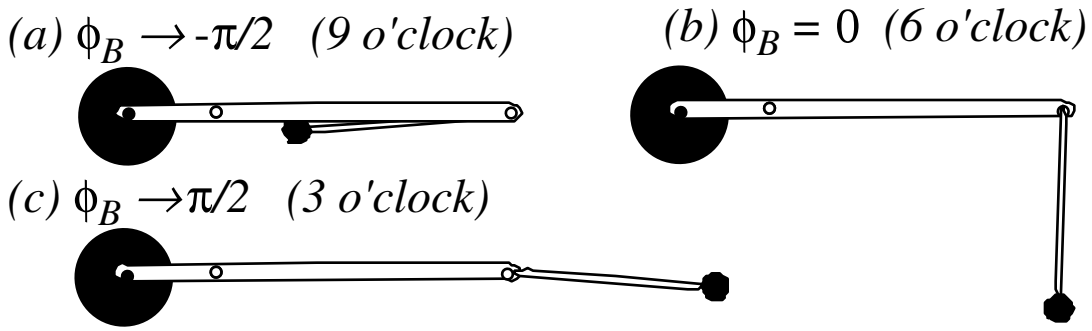

Fig. 9 Extreme beam-relative coordinate positions.

If the rope or lever-ℓ is tucked in along the main beam at 9 o'clock then ϕ_B=$-\pi/2$ so (49b) reduces to

$$\phi_B = \frac{-\pi}{2}: \begin{cases} \Lambda = MR^2\dot\theta_{-\pi/2} \\ 2E = MR^2\dot\theta_{-\pi/2}^{\,2} + mr^2\left(\dot\phi_{-\pi/2} - \dot\theta_{-\pi/2}\right)^2 \end{cases} \quad or: \begin{cases} \Lambda = MR^2\omega \\ 2E = MR^2\omega^2 \end{cases} \text{ For: } \omega = \dot\theta_{-\pi/2} = \dot\phi_{-\pi/2} \tag{50a}$$

We will assume ϕ_B=$-\pi/2$ is the initial position where both angles have the same initial velocity ω. If the rope or lever-ℓ is normal to the main beam (at 6 o'clock in Fig.5 or Fig. 9b) then ϕ_B=0 and the equation (49b) reduces to

$$\phi_B = 0: \begin{cases} \Lambda = MR^2\dot\theta_0 + mr^2\left(\dot\phi_0 + \dot\theta_0\right) \\ 2E = MR^2\dot\theta_0{}^2 + mr^2\left(\dot\phi_0{}^2 + \dot\theta_0{}^2\right) \end{cases} \tag{50b}$$

If the rope or lever-ℓ is stretched out along the main beam at 3 o'clock then ϕ_B=$\pi/2$ so (49b) reduces to

$$\phi_B = \pi/2: \begin{cases} \Lambda = MR^2\dot\theta_{\pi/2} + 2mr^2\left(\dot\phi_{\pi/2} + \dot\theta_{\pi/2}\right) \\ 2E = MR^2\dot\theta_{\pi/2}{}^2 + mr^2\left(\dot\phi_{\pi/2} + \dot\theta_{\pi/2}\right)^2 \end{cases} \tag{50c}$$

We take *9 o'clock* (ϕ_B=$\pi/2$) to be a launch position which, presumably, would provide the greatest velocity for the projectile m. According to (22) and (23a) mass m has the following *KE* and speed v.

$$KE(m)=\frac{1}{2}mr^2\left(\dot\phi^2+\dot\theta^2+2\dot\phi\dot\theta\sin\phi_B\right)=\begin{cases}\frac{1}{2}mr^2\left(\dot\phi-\dot\theta\right)^2 & \left(\text{For: } \phi_B=-\frac{\pi}{2}\right)\\ \frac{1}{2}mr^2\left(\dot\phi^2+\dot\theta^2\right) & \left(\text{For: } \phi_B=0\right)\\ \frac{1}{2}mr^2\left(\dot\phi+\dot\theta\right)^2 & \left(\text{For: } \phi_B=\frac{\pi}{2}\right)\end{cases} \qquad (51a)$$

where final projectile speed is

$$v=\sqrt{\frac{2KE(m)}{m}} \qquad (51b)$$

Equating final *(Λ,E)* in (50c) to initial *(Λ,E)* in (50a) gives easily solved equations.

$$\omega-\dot\theta_{\pi/2}=\frac{2mr^2}{MR^2}\left(\dot\phi_{\pi/2}+\dot\theta_{\pi/2}\right) \qquad (52a)$$

$$\omega^2-\dot\theta_{\pi/2}{}^2=\frac{mr^2}{MR^2}\left(\dot\phi_{\pi/2}+\dot\theta_{\pi/2}\right)^2 \qquad (52b)$$

Dividing (52b) by (52a) gives a linear relation.

$$\omega+\dot\theta_{\pi/2}=\frac{1}{2}\left(\dot\phi_{\pi/2}+\dot\theta_{\pi/2}\right) \quad \text{or:} \quad \dot\phi_{\pi/2}=\dot\theta_{\pi/2}+2\omega \qquad (52c)$$

If the main beam is quite massive compared to the projectile *(M>>m)*, then its angular velocity may remain fairly constant, so its initial velocity $\dot\theta_{-\pi/2}\equiv\omega$ is not significantly greater than the final velocity $\dot\theta_{\pi/2}\cong\omega$. Then by (52c) the projectile lever or rope ℓ has final angular velocity *3 times* that of the beam: $\dot\phi_{\pi/2}\cong 3\omega$.

Substituting this approximate value into the *KE* and speed formula (51) for $\phi_B=\pi/2$ gives a kinetic energy that is *sixteen times* that of a mass sitting on the end of the *r*-beam.(*m* would ride there in a simple catapult.)

$$KE(m)=\frac{1}{2}mr^2\left(\dot\phi_{\pi/2}+\dot\theta_{\pi/2}\right)^2\cong\frac{1}{2}mr^2(4\omega)^2=16\frac{mr^2\omega^2}{2} \qquad (53a)$$

This amounts to a projectile velocity (51b) that approaches four times the speed of the beam tip.

$$v_{final}=\sqrt{\frac{2KE(m)}{m}}\cong 4\omega r \qquad (53b)$$

This is consistent with the result $v=\omega\left(r_b+\ell+2\sqrt{\ell r_b}\right)$ in (7) for a constant-ω model with $r_b=\ell$ in the case for which it starts full-cocked in a *9 o'clock* initial position and releases at *3 o'clock*.

However, the present model tells how much angular velocity the beam loses. Substituting $\dot\phi_{\pi/2}$ from (52c) into (52a) shows that the final beam angular velocity $\dot\theta_{-\pi/2}$ can be reduced to zero or negative values.

$$\omega-\dot\theta_{\pi/2}=\frac{2mr^2}{MR^2}\left(2\omega+2\dot\theta_{\pi/2}\right) \qquad \text{or:} \qquad \dot\theta_{\pi/2}=\frac{1-\frac{4mr^2}{MR^2}}{1+\frac{4mr^2}{MR^2}}\omega \qquad (54)$$

The case $MR^2=4mr^2$ is interesting because the beam is stopped completely while giving 100% of its energy to the projectile. With $\dot{\theta}_{\pi/2} \cong 0$ the projectile angular velocity ends up *2 times* that of the initial beam angular velocity ($\dot{\phi}_{\pi/2} \cong 2\omega$ according to (52c)) instead of *3 times* which is the limit for small *m*.

These results are reminiscent of those for a super-ball-pen or tower first described about thirty years ago [7]. In those experiments, a superball of mass *M* descends to the floor with a smaller object *m* riding on top. If the rider is of negligible mass *m* compared to *M*, it is bounced skyward at three times the initial contact velocity. But if mass *m* is just large enough (that is *m=M/3*) to stop *M* and take all its energy, then it is thrown skyward at just twice the initial velocity.

Relating the simple gravity-free kinetic theory above to a gravity driven trebuchet is problematic, to say the least. One is left to devise a number of estimation schemes. For example, the initial beam angular velocity ω could be derived from the average velocity $\left\langle \bar{\dot{\theta}} \right\rangle$ of a gravity driven beam with projectile *m* fixed at some average position, say at the *6 o'clock* position. For *m/M<<1* this can be (over)estimated to be the average angular velocity of a pendulum of length *R* falling angle *π/2* from the *9 o'clock* initial position in Galileo's approximation.

$$\omega = \left\langle \bar{\dot{\theta}} \right\rangle \sim \sqrt{\frac{g}{R}} \tag{55}$$

The reproductions of 12th century trebuchets in Ref. [2] were based on drawings from ingeniums used in the siege of Kenilworth. The modern-day ingeniators used twelve to thirteen thousand pounds of sand to throw a 250 pound stone ball, that is, *M/m~50*. Had they used the criterion $MR^2=4mr^2$ for *100%* energy transfer from (54) their trebuchet would have a ratio *r/R = √50/2=3.5* of the throwing beam to driving beam radii. Instead, the drawings show that *ℓ~r~42 ft.* is about 3.7 times the driving radius *R* of the sand box *M*. Using (52) to (55) with 100% energy transfer assumption we find the following approximate launch velocity.

$$v_{final} \cong 2\omega r = 2\sqrt{\frac{g}{R}}\, r = 2\sqrt{\frac{32}{42/3.5}}\, 42 = 137\ ft/sec. = 94\ mph \tag{56}$$

As one might expect, this 100% estimate is below the *100* to *120 mph.* velocities achieved in Ref. {2}. By assuming the correct ratio of radii in using (52) to (55), one can bring the estimate closer.

11. Advanced trebuchet mechanics

Accurate theoretical simulation or prediction of trebuchet launches such as those described in Ref. [2] will generally require analytical and numerical techniques such as those described in Sec. 8. For one thing, Ref. [2] described a trebuchet with wheels that moved forward and thereby added translation velocity to the projectile. This involves a translation degree of freedom *x* and carriage mass μ as shown in Fig. 10. Each degree of freedom makes analytical solutions more difficult and numerical simulation more necessary.

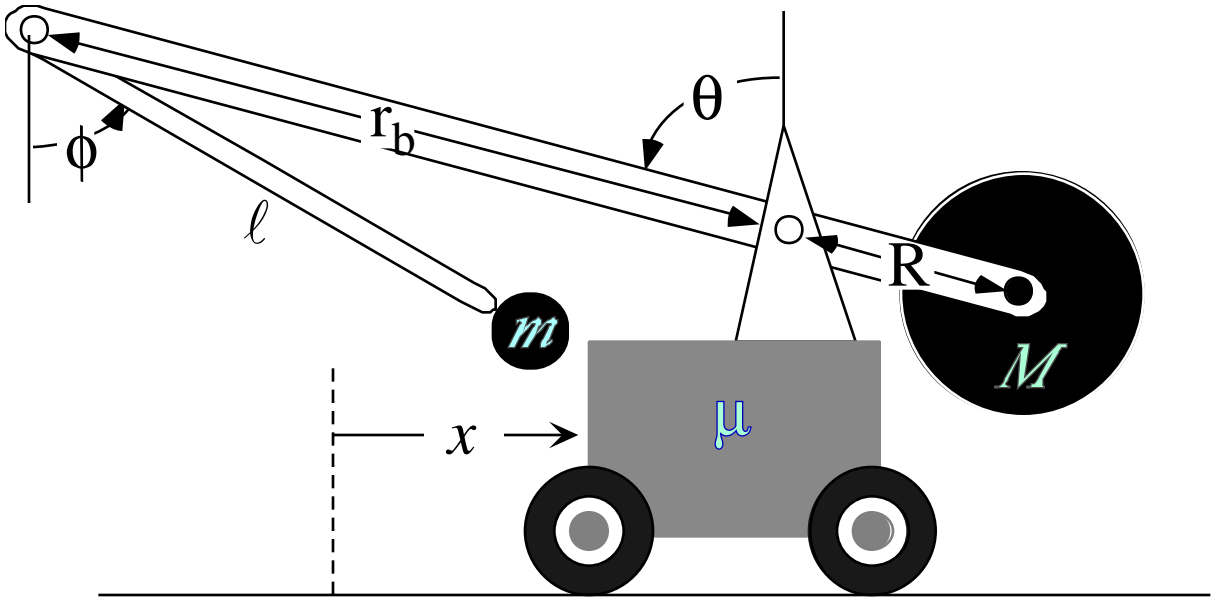

Fig. 10 Trebuchet with translation uncoil and recoil allowed.

As long as numerical techniques are used, one may as well improve the stick-and-ball pendulum models so they account for the compound pendulums whose radii of gyration are generally smaller than the geometric radii. The discrepancy between inertial and geometric radii is most obvious in discussions of the analogy with tennis racquet dynamics involving Fig. 3c, but most trebuchets need this correction, as well.

Modern materials and analysis also open the possibility of serial-segment trebuchets such as the triple segmented device sketched in a simulation shown by Fig. 11. A trebuchet with more than two moving parts is easily capable of exceeding the upper limit of $\dot{\phi}_{-\pi/2} \cong 3\omega$ and $v_{final}=4\omega r$ that limits two-part machines. In Ref. 5 it was shown how superball towers with n=3, 4, 5,... parts can, in principle, achieve very high velocity.

A multi-segment trebuchet is analogous to a baseball pitch and a tennis serve, the latter of which is achieving extraordinary velocities in world-class play. More simply, the multi-segment trebuchet is like a (sometimes dangerous) "crack-the-whip" game played by a chain of children on skates. More to the point, such a device could be modeled after a bull-whip.

One wonders, "Could a gravity driven multi-trebuchet actually throw a massive object faster than the speed of sound?" Certainly a spring, motor or hand driven device can exceed 700 mph. For centuries it was done daily using bullwhips on Southern and Latin American cattle ranches. (It is said that semi-tropical cowhands were called "Crackers" for this reason.) But, getting such kinetic energy solely from a large mass potential *Mgh* would require some extraordinary physics and engineering. The PE of *M=50 kg* mass raised *1 m* equals the KE of a *m=1 gm* mass traveling *v=1km/sec*. or *2,215 mph* or about *Mach 3*, according to a simple energy equation.

$$v_{final} = \sqrt{\frac{2Mgh}{m}} = \sqrt{\frac{2 \cdot 50kg \cdot 10ms^{-2} \cdot 1m}{10^{-3}kg}} = 10^3 ms^{-1}. \qquad (57)$$

This is reduced to *Mach 1* for a *1 gm* mass powered by a *5.5 kg* mass or a *0.18 gm* mass powered by a one kilogram weight. The latter begins to sound practical, but it assumes that 100% transfer is possible for each

trebuchet segment. However, it remains to be seen if the 2-segment analysis leading to (52) through (54) may be applicable to a multi-segmented device.

Instead, a better model for a multi-segment device may be that of a bull-whip wave traveling from the heavier end toward the lighter segments and gradually increasing velocity at each joint. Again, this is very similar to the dynamics of the superball tower analyzed in Ref. [7]. Under the right conditions the independent 2-particle collision model was applicable to *N*-superball amplification. Such multi-stage dynamics have a relativistic version in stellar models of super-novae and the resulting kinetic transfer is called super-elastic-bounce.[8]

Such a complex and high speed system is likely to require numerical simulation to accompany its construction and engineering. Optimal control theory techniques should help find the best designs and initial settings. A student using a computer can try more different settings in five minutes than all the ingeniators of the world did in five centuries! High speed digital video tracking of real lab devices can be used to calibrate and check the numerical simulations each time another segment is added to the device. Bending of segments may also be important as it certainly was for the great thirty-ton wooden trebuchets of the 11-th century.

Each increase in speed will bring even larger increases in frictional loss of energy. Friction can only be modeled semi-emperically so the video input coupled with numerical computer graphical techniques will become more essential as the device gains complexity. (Perhaps the whole experiment could be done in a vacuum, but what fun would it be if you can't hear the "Crack!")

12. Conclusion

The trebuchet dynamics have been shown to be far more valuable to physics and physics education than previously realized. Connections with fundamental human motions at work and play have been discussed semi-quantitatively. Methods for approximately analyzing trebuchet-like energy transfer have been given and range in complexity from simple energy or momentum kinetics to equations of Lagrange, Hamilton, and Riemann-Christoffel. Interestingly, only the Riemann-Christoffel equations are directly amenable to Runga-Kutta numerical solution. Numerics are needed for developing advanced trebuchets such as the proposed supersonic throwing device.

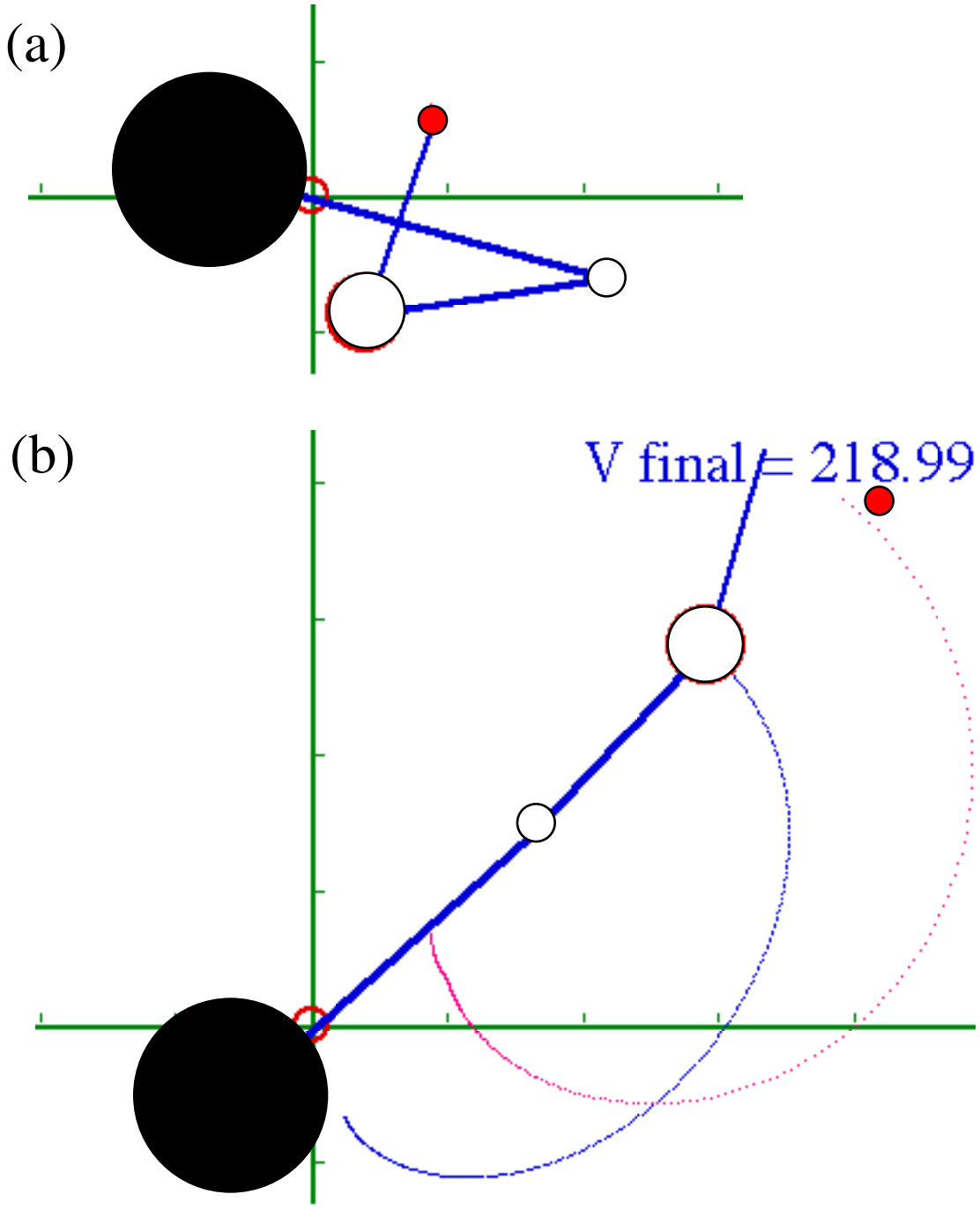

Fig. 11 Non-optimized example of simulated 3-stage trebuchet dynamics .(a) Initial position state. (b) Just after launch.

Acknowledgment

We thank the reveiwer Frank Munley for his extensive suggestions. This research was supported in part by a Fulbright College Teaching Innovation Grant and a 1999 Charles and a Nadine Baum Teaching Improvement Grant .

References

1. Paul E. Chevedden, Les Eigenbrod, Vernard Foley, and Werner Soedel, *"The Trebuchet"*, *Scientific American* **273**, 66-71 (July 1995).
2. Evan Hadingham and Patrick Ward, *"Ready, Aim, Fire!"*, *Smithsonian* (January 2000) p. 80.
3. Ref. 1 p.69.
4. Literature search beyond the above references reveals a number of exercises in computer *synthesis* of the trebuchet, but practically no physical *analysis*. It is this imbalance that we seek to begin correcting. The ingenium was invented by engineers. (Or, they were invented by it!) Physicists seem quite late coming to this party.
5. William G. Harter, *Classical Mechanics With a Bang!* (U of A Course 5301 Text (Unpublished)).
6. Jon Mathews and R. L. Walker, *Mathematical Methods for Physics* (Benjamin, NewYork, 1964) p. 189; The mechanical analogy is discussed extensively in Ref.5 and in a companion text: *Quantum Theory for the Computer Age* (U of A Course 5103 Text (Unpublished)).
7. Class of W. G. Harter, "*Velocity Amplification in Collision Experiments Involving Superballs*," *Am. J. Phys.* **39**, 656 (1971) (A class project which received NBC news coverage).
8. S. E. Wollsley, and M. M. Phillips, "*Super-Nova 1987A!*" *Science* **240**, 750 (May 1988).

Figure Captions

Fig. 1 The elementary ground-fixed Trebuchet

Fig. 2 Galileo's Supposed Problem: Solve the trebuchet

Fig. 3 Example of elementary trebuchet dynamics and qualitative analogy with tennis racquet swing

Fig. 4 Example of elementary "flinger" dynamics and qualitative analysis

Fig. 5 Comparing rotating frame dynamics of (a) trebuchet and (b) flinger for similar dimensions

Fig. 6 Simple experiments for comparing dynamics of (a) trebuchet and (b) flinger for similar dimensions.

Fig. 7 Two (very different) types of accelerated pendulum resonance .

Fig. 8 Trebuchet Coordinates
(a) Glossary of possible coordinate angles for trebuchet (All values shown are positive.)

(b) Left-handed (θ,ϕ)-manifold hilighting $\theta=0$ and $\phi=3\pi/4$ lines.

(c) Right-handed (θ,ϕ)-manifold hilighting $\theta=-\pi/4$ and $\phi=\pi$ lines

(d) Left-handed (θ,ϕ_B)-manifold hilighting $\theta=0$ and $\phi_B=\pi/4$ lines

(e) Right-handed (θ,ϕ_B)-manifold hilighting $\theta=-\pi/4$ and $\phi_B=3\pi/4$ lines

Fig. 9 Extreme beam-relative coordinate positions.

Fig. 10 Trebuchet with translation uncoil and recoil allowed.

Fig. 11 Non-optimized example of simulated 3-stage trebuchet dynamics
.(a) Initial position state. (b) Just after launch.